

When cold, dense quarks in 1 + 1 and 3 + 1 dimensions are not a Fermi liquid

Marton Lajer,¹ Robert M. Konik,¹ Robert D. Pisarski²,³ and Alexei M. Tsvelik¹

¹*Division of Condensed Matter Physics and Material Science, Brookhaven National Laboratory, Upton, New York 11973-5000, USA*

²*Department of Physics, Brookhaven National Laboratory, Upton, New York 11973, USA*



(Received 22 December 2021; accepted 4 February 2022; published 30 March 2022)

We analyze the behavior of quarks coupled to a $SU(N_c)$ gauge theory in 1 + 1 dimensions. In the limit of strong coupling, the model reduces to a Wess-Zumino-Novikov-Witten (WZNW) model. At nonzero density, excitations near the Fermi surface form a non-Fermi liquid. With N_f flavors, the finite density of quarks reduce to a free $U(1)$ field, which governs fluctuations in baryon number, together with a WZNW $SU(N_f)$ nonlinear sigma model at level N_c , from the pion/kaon modes. We compute the singularity in the charge susceptibility at the Fermi surface and the attendant power-law correlations. We suggest that this is relevant to the quarkyonic regime of cold, dense QCD in (3 + 1) dimensions, in the limit that the Fermi surface is covered by many small patches, and the theory is effectively one dimensional. In this regime the dominant excitations near the Fermi surface are not baryons, but gapless bosonic modes.

DOI: [10.1103/PhysRevD.105.054035](https://doi.org/10.1103/PhysRevD.105.054035)

I. INTRODUCTION

The behavior of QCD at nonzero temperature and density is of fundamental interest. Since numerical simulations on the lattice are not possible for three (or more) colors at nonzero density, and as quantum computers are far from able to compute the behavior of cold, dense QCD, it is useful to study analytically tractable models, even those in fewer dimensions, that may reflect the essential features of the underlying physics.

At low density, nuclear matter is well described by effective theories of nucleons. This describes the theory up to and for some region beyond saturation density [1–8]. Conversely, at very high density, perturbation theory in the QCD coupling applies [9–17]. Previously it has been argued that at intermediate densities there is a quarkyonic regime, where the free energy is that of an interacting theory of quarks and gluons, but near the Fermi surface, the excitations are confined [18–32]. This is the regime that we wish to concentrate upon in this paper.

It was shown in Refs. [21,31,33–36] that the quarkyonic regime is a critical state which shares many aspects with systems in (1 + 1) dimensions. We explore this analogy further in this paper.

In 1 + 1 dimensions the gauge coupling g has dimensions of mass, so weak coupling is the regime where the

quark mass is large relative to g . We concentrate on strong coupling, where the quark masses are small relative to g . For vanishing bare quark masses, non-Abelian bosonization demonstrates that the gapped color sector decouples. In the vacuum, and at energies small relative to the gauge coupling, the quarks are confined and the low-energy degrees of freedom are gapless $U(1)$ and $SU(N_f)_{N_c}$ Wess-Zumino-Novikov-Witten (WZNW) meson fields. There are baryons, but these are not coherent excitations, but nonlocal combinations of the mesonic fields. At small but finite quark mass, the color sector can be integrated out, and generate perturbations in the low-energy sector.

In this paper we consider whether a non-Fermi liquid exists in QCD in 1 + 1 dimensions at nonzero density. The Nambu-Jona-Lasinio (NJL) model was studied in 1 + 1 dimensions in Ref. [37]. At nonzero density, even at nonzero bare quark mass sectors with different symmetry decouple. We argue that this decoupling remains valid for QCD. In the NJL model, there are two regimes at nonzero density: a state with gapped flavor and gapless $U(1)$ excitations at low density, and a critical state at higher density. The baryons are formed from the $U(1)$ and flavor fields, but in both regimes the spectral function for a single baryon never exhibits a sharp peak, as the baryons are “incoherent.” This is unlike the typical Fermi liquid, where the spectral function has a sharp peak, which allows for the consistent definition of quasiparticles. In the NJL model, the behavior of baryon Green’s functions changes between the two regimes. At low density, both the flavor sector and baryons are gapped, and baryon correlation functions are exponentially damped. In contrast, the high-density phase is critical, as the baryon

Published by the American Physical Society under the terms of the Creative Commons Attribution 4.0 International license. Further distribution of this work must maintain attribution to the author(s) and the published article’s title, journal citation, and DOI. Funded by SCOAP³.

spectral function is gapless, and baryon correlation functions fall off as a power law. This can be termed a strange metal.

To establish the density at which a strange metal appears depends upon the details of the low-energy theory. We argue that in $1 + 1$ dimensions, the low-energy theory is the same for both the NJL model and QCD. At sufficiently low density the quark mass term generates a relevant perturbation in the flavor sector. For this to happen the Luttinger parameter in the $U(1)$ sector must exceed a critical value determined by the quark mass, the chemical potential, and depends upon how many flavors, N_f , and colors, N_c , there are. We extract this dependence for two cases. First, for an arbitrary N_c and a single flavor, $N_f = 1$ [38–43]. Second, for two colors and two flavors, $N_c = N_f = 2$. We expect that the behavior for other values of N_c and N_f is qualitatively similar, although the details certainly change.

Our methods are only useful in the strong coupling regime of light quarks. It is possible that for a low density of heavy quarks, QCD in $(1 + 1)$ dimensions is no longer a Luttinger liquid, and baryon correlation functions are gapped, like the low-density regime of the NJL model [37]. Heavy quarks inevitably form a Luttinger liquid at high density, though, once the mass term is negligible relative to the chemical potential. It is also natural to conjecture that for any mass, baryons are incoherent at all densities.

A gauge theory in $1 + 1$ dimensions coupled to fermions in the adjoint representation has been studied in Refs. [44,45]. For massless fields, at nonzero density the theory is again a strange metal [44], described by a supersymmetric WZNW model. This is considerably more complicated than the simple Luttinger liquid which emerges for quarks in the fundamental representation.

While the phenomenology of QCD in $(1 + 1)$ dimensions is interesting in and of itself, here we are primarily motivated by its consequences to quarkyonic matter in $(3 + 1)$ dimensions. For ordinary nuclear matter, the excitations near the Fermi surface are baryons, and are typically gapped, being Bogolyubov quasiparticles of either the superfluid or superconducting state. While the gaps are small, on the order of a few MeV, transport coefficients are exponentially suppressed at temperatures less than these gaps. As the density increases, nuclear matter is quarkyonic, and forms a smectic liquid crystal [21,33,34]. The Fermi surface of the theory spontaneously divides itself into patches, where the propagators for gapless bosons are anisotropic, and differ between the direction of the condensate and transverse fluctuations. As was discussed previously [21,33,34], the solution is stable when there are many patches, when the net quark density is large. Then the theory for each patch is effectively one dimensional, and the coherent excitations at low energy are then not baryons, but gapless bosons, both Abelian and non-Abelian, with a dispersion relation which is quasi-one-dimensional. These bosonic modes are color singlets, related to a low-energy WZNW model of the

flavor degrees of freedom. Our arguments are qualitative, as our purpose is simply to emphasize that the quarkyonic matter is a non-Fermi liquid. This is of direct consequence for the transport properties of cold quarkyonic matter.

In Sec. II we analyze QCD, coupled to quarks in the fundamental representation, in $(1 + 1)$ dimensions. The effective Wess-Zumino-Witten Lagrangian at low energy is given in Sec. II B, and extended to nonzero density in Sec. III. Detailed computations of the Luttinger parameter are given in Secs. III A and III B, while the properties of the strange metal for $N_c = 3$, $N_f = 2$ are detailed in Sec. III C. In Sec. IV we outline the possible relation to cold, dense QCD in $(3 + 1)$ dimensions. Appendixes include a review of the quantum Ising model, Appendix A; of the thermodynamic Bethe ansatz, Appendix B; the numerical analysis for a single flavor, Appendix C; and details of the perturbative calculation, Appendix D.

II. DENSE MATTER IN $(1 + 1)d$ QCD

As we have discussed above, some physical aspects of $(3 + 1)d$ quarkyonic state are essentially $(1 + 1)d$ in character. Therefore we will start our discussion from the pure $(1 + 1)d$ case.

We will work with the premise that all physical states in $(1 + 1)d$ are color singlets. Thus to obtain an effective low-energy description, we have to integrate out the color degrees of freedom. The effective action and operators should be projected onto the color singlet ground state. One way to approach the problem is to use non-Abelian bosonization and the notion of conformal embeddings. Here we will use the fact that the Hamiltonian of massless Dirac fermions of N_c colors and N_f flavors can be decomposed into three commuting Wess-Zumino-Novikov-Witten Hamiltonians describing the $U(1)$, the color, and the flavor sectors [38–43].

In the NJL model there is a local interaction between color currents and the color sector is gapped [37]. In QCD, integrating out the gluons generates a long-range interaction between the color currents; thus it is reasonable to assume that the color sector remains gapped. In $(1 + 1)d$, the gap is of order $\Lambda_{\text{QCD}} \sim g$. For massless quarks, the color currents commute with the charge and flavor sectors, leaving a $U(N_f)_{N_c}$ WZNW model at low energies.

There are issues which need clarification related to the projection of the observables. They emerge even for the case of massless quarks or for the dense phase where the mass term becomes irrelevant. As was noted in the earlier works on $(1 + 1)d$ QCD, there are various observables, including the mass term, which do not factorize into a product of local fields from the color and flavor sectors. This was noticed already in Ref. [42] where it was stated that although the Hamiltonian of $(1 + 1)d$ QCD with $N_f, N_c \geq 2$ can be decomposed via a conformal embedding into three commuting parts consisting of WZNW models acting, respectively,

on the charge, the flavor and the color sectors, the mass term cannot be written as a product of mutually local fields of these models. In fact, this is a common problem for conformal embeddings. After integrating out the high-energy degrees of freedom, the color singlet operators can be expressed as local fields of the low-energy field theory, which is the $U(N_f)_{N_c}$ WZNW model. Below we discuss the details of the projection for two particular cases: a single flavor, $N_f = 1$, for arbitrary N_c , and $N_c = N_f = 2$. The conformal embedding is done using Abelian bosonization, as in Ref. [46]. The conclusion is that after one executes a projection onto the color singlet vacuum, the corresponding fields are expressible in terms of the local fields of the charge and flavor sector.

The QCD Lagrangian with the quarks in the fundamental representation of the $SU(N_c)$ color group is

$$L = \int d^D x \left[-\frac{1}{8\pi g^2} \text{tr} F^{\mu\nu} F_{\mu\nu} + \bar{q}_{f,\sigma} \gamma^\mu D_{\mu,\sigma\sigma'} q_{f,\sigma'} + m \bar{q}_{f,\sigma} q_{f,\sigma} \right], \quad (1)$$

where the covariant derivative is defined as

$$D_\mu^{\sigma\sigma'} = \delta^{\sigma\sigma'} \partial_\mu - i A_\mu^{\sigma\sigma'}. \quad (2)$$

The quark fields \bar{q}, q carry $f = 1, \dots, N_f$ flavor and $\sigma = 1, \dots, N_c$ color indices and the color Yang-Mills field is

$$F_{\mu\nu} = \partial_\mu A_\nu - \partial_\nu A_\mu - i[A_\mu, A_\nu]. \quad (3)$$

In $(1+1)d$ one can choose the gauge where $A_x = 0$ and integrate out the color Yang-Mills field. Then after a suitable choice of the gamma matrices, we arrive at the following Hamiltonian for $(1+1)d$ QCD:

$$H = \sum_{f=1}^{N_f} \sum_{\sigma=1}^{N_c} \int dx \left[-i R_{f,\sigma}^+ \partial_x R_{f,\sigma} + i L_{f,\sigma}^+ \partial_x L_{f,\sigma} - m (R_{f,\sigma}^+ L_{f,\sigma} + L_{f,\sigma}^+ R_{f,\sigma}) \right] - \pi g^2 \int dx dy J_0^a(x) |x-y| J_0^a(y), \quad (4)$$

where

$$J_0^a = J_R^a + J_L^a, \quad (5)$$

$$J_R^a = \sum_{f=1}^{N_f} R_{f,\sigma}^+ t_{\sigma\sigma'}^a R_{f,\sigma'}, \quad J_L^a = \sum_{f=1}^{N_f} L_{f,\sigma}^+ t_{\sigma\sigma'}^a L_{f,\sigma'}. \quad (6)$$

Here t^a matrices are generators of the $SU(N_c)$ algebra and R, L are the right- and left-moving components of the q -spinor field. The currents of the right- and left-moving quarks $J_{R,L}$

obey a $SU(N_c)_{N_f}$ Kac-Moody algebra. (For a comprehensive review of non-Abelian bosonization, see Ref. [47].) One can rewrite the Hamiltonian as the sum of three mutually commuting parts plus the mass term, which mixes them all:

$$H = H[U(1)] + H_{\text{color}} + H_{\text{flavor}} + \text{mass}, \quad (7)$$

where $H[U(1)], H_{\text{flavor}}$ are Hamiltonians of the WZNW models of the corresponding groups. H_{color} is the $SU(N_c)_{N_f}$ WZNW model perturbed by the current-current interaction of Eq. (4). These Hamiltonians are expressed in terms of the $U(1), SU(N_c)_{N_f}$, and $SU(N_f)_{N_c}$ Kac-Moody currents.

For $N_f > 1$ at zero quark mass the Hamiltonian is separated into three commuting parts. The mass term however violates this separation. As was mentioned in the Introduction, the corresponding density operator cannot be even factorized into a product of mutually local operators acting on the corresponding Hilbert spaces. This may lead to difficulties in formulating the low-energy theory in the strong coupling limit. We argued in Ref. [37] for the NJL model that the issue is resolved once the Hamiltonian is projected on the color singlet ground state of the color sector. To elucidate the nature of the issues involved we will consider both the case $N_f = 1$ and the case of $N_c = N_f = 2$. Here one can treat the conformal embedding using Abelian bosonization, as it was done, for example, in Ref. [46].

A. Low-energy theory for $N_f = 1$

We begin with the simplest case, that of a single flavor, $N_f = 1$. We start with Abelian bosonization of the free quarks and use the standard bosonization rules for the operators of right- and left-moving quarks ($\sigma = 1, \dots, N_c; f = 1, \dots, N_f$):

$$R_{f,\sigma} = \frac{1}{\sqrt{2\pi}} \xi_{f,\sigma} \exp[i\sqrt{4\pi}\varphi_{f,\sigma}], \quad L_{f,\sigma} = \frac{1}{\sqrt{2\pi}} \xi_{f,\sigma} \exp[-i\sqrt{4\pi}\bar{\varphi}_{f,\sigma}], \quad (8)$$

where $\varphi_n, \bar{\varphi}_n$ ($n = (f, \sigma)$) are chiral bosonic fields governed by the Gaussian action (from now on we will work in Euclidean time),

$$S_{\text{Gauss}} = \frac{1}{2} \sum_{n=(f,\sigma)} \int d\tau dx (\partial_\tau \varphi_n)^2 + (\partial_x \varphi_n)^2. \quad (9)$$

The chiral vertex operators, i.e. $\exp[i\sqrt{4\pi}\bar{\varphi}_{f,\sigma}]$, are assumed to be normal ordered and have a normalization determined by

$$\langle\langle e^{-i\sqrt{4\pi}\varphi_{f,\sigma}(\tau,x)} e^{i\sqrt{4\pi}\varphi_{f,\sigma}(0,0)} \rangle\rangle = \frac{1}{\tau - ix}. \quad (10)$$

Finally ξ_n are anticommuting Klein factors that ensure this bosonic representation of the quarks anticommutes.

This case can be treated explicitly for any N_c . Bosonization yields

$$S = S_{\text{Gauss}} + \int d\tau dx (V_{\text{Cartan}} + V_{\text{off-diag}}), \quad (11)$$

$$V_{\text{off-diag}} = \sum_{a>b} \int dy \frac{g^2}{4\pi} |x-y|^{-1} \{ \cos[\sqrt{4\pi}[\varphi_{ab}(x) - \varphi_{ab}(y)]] + \cos[\sqrt{4\pi}[\bar{\varphi}_{ab}(x) - \bar{\varphi}_{ab}(y)]] - 2|x-y|^2 \cos[\sqrt{4\pi}[\varphi_{ab}(x) + \bar{\varphi}_{ab}(y)]] \} \quad (13)$$

with $\varphi_{ab} = \varphi_a - \varphi_b$.

The form of the effective potential (12) is suggestive of the confinement: since it is not periodic in the fields, it does not allow topological excitations for any field configurations except one. The only soft mode remaining is the one

$$\Phi_U = \frac{1}{\sqrt{N_c}} \sum_a \Phi_a, \quad (14)$$

which does not enter into V . The ground state of (11) corresponds to all fields being equal; projecting the mass term on this vacuum we get the sine-Gordon model with renormalized mass term:

$$\mathcal{H}_{\text{eff}} = \frac{1}{2} \{ \Pi^2 + (\partial_x \Phi_U)^2 \} + 2 \frac{\tilde{m}}{2\pi} \left[1 - \cos \left(\sqrt{\frac{4\pi}{N_c}} \Phi_U \right) \right]. \quad (15)$$

Naturally, the projection assumes that the energy scale generated by the mass term is much smaller than the energies of the mesonic fields. Even for a single flavor, the complete bosonized form of QCD involves a set of N_c coupled sine-Gordon models, as first derived by Baluni [38–43]. Besides the $U(1)$ field Φ_U , there are also color singlet excitations above Λ_{QCD} , involving fluctuations of individual fields Φ_a around the minimum of the potential. By going to energies below the scale of the gauge coupling, all of these massive degrees of freedom can be ignored. This simplifies the analysis considerably.

B. Low-energy theory for $N_f = N_c = 2$

For $N_c = N_f = 2$ the indices σ and f take the values $\sigma = \pm 1, f = \pm 1$. The Gaussian models in Eq. (9) have total central charge $c = 4$. Our goal is to rearrange the

$$V_{\text{Cartan}} = -\pi g^2 \int dy |x-y| \partial_x \Phi_a (\delta_{ab} - 1/N_c) \partial_y \Phi_b = g^2 \Phi_a (\delta_{ab} - 1/N) \Phi_b, \quad (12)$$

where S_{Gauss} is the Gaussian action (9), we have introduced nonchiral bosons $\Phi = \varphi + \bar{\varphi}$, and the off-diagonal part is given by

fields into groups with central charges 1, 3/2 and 3/2 corresponding to the $U(1)$, $SU(2)_2$ flavor and $SU(2)_2$ color sectors. The next step is to introduce new bosonic fields, $\varphi_U, \varphi_F, \varphi_c$, and φ_{cF} , defined by

$$\begin{aligned} \varphi_{f,\sigma} &= \frac{1}{2} (\varphi_U + f\varphi_F + \sigma\varphi_c + f\sigma\varphi_{cF}), \\ \bar{\varphi}_{f,\sigma} &= \frac{1}{2} (\bar{\varphi}_U + f\bar{\varphi}_F + \sigma\bar{\varphi}_c + f\sigma\bar{\varphi}_{cF}). \end{aligned} \quad (16)$$

This transformation leaves the bosonic action of Eq. (9) covariant. The derivatives of fields $\varphi_U, \bar{\varphi}_U$ are $U(1)$ currents describing smooth fluctuations of the particle density. From other bosonic fields we construct the other currents—generators of the $SU(2)_2$ flavor and color Kac-Moody algebras. For instance, the color right- and left-moving color currents

$$\begin{aligned} J_R^a &= \frac{1}{2} \sum_{f=1}^2 R_{f,\sigma}^+ \tau_{\sigma,\sigma'}^a R_{f,\sigma'} = \epsilon_{abc} \chi_R^b \chi_R^c, \\ J_L^a &= \frac{1}{2} \sum_{f=1}^2 L_{f,\sigma}^+ \tau_{\sigma,\sigma'}^a L_{f,\sigma'} = \epsilon_{abc} \chi_L^b \chi_L^c, \end{aligned} \quad (17)$$

where τ^a are Pauli matrices and the labels are $a = (1c, 2c, 3c)$, are expressed in terms of Majorana fermions. The Majorana fermions describing the color sector are related to the following chiral bosonic fields via the relations:

$$\begin{aligned}
\chi_{R,1c} &= \frac{1}{\sqrt{\pi}} \xi_c \sin(\sqrt{4\pi}\varphi_c), & \chi_{R,1F} &= \frac{1}{\sqrt{\pi}} \xi_F \cos(\sqrt{4\pi}\varphi_F), \\
\chi_{R,2c} &= \frac{1}{\sqrt{\pi}} \xi_c \cos(\sqrt{4\pi}\varphi_c), & \chi_{R,2F} &= \frac{1}{\sqrt{\pi}} \xi_F \sin(\sqrt{4\pi}\varphi_F), \\
\chi_{R,3c} &= \frac{1}{\sqrt{\pi}} \xi_{cF} \cos(\sqrt{4\pi}\varphi_{cF}). & \chi_{R,3F} &= \frac{1}{\sqrt{\pi}} \xi_{cF} \sin(\sqrt{4\pi}\varphi_{cF}).
\end{aligned} \tag{18}$$

The left-moving ones are related similarly to the corresponding $\bar{\varphi}$ fields. The Cartan current J^3 is understood in the regularized sense, i.e. it corresponds to the derivative of the field φ_c . Likewise one can introduce the triad of the Majoranas to represent the $SU(2)_2$ flavor sector:

Please note that the bosonic field cF takes part in both the color and the flavor sectors since it enters in the Majorana fermions $3c$ and $3F$. The mass term in terms of the transformed bosons becomes

$$\begin{aligned}
\sum_{f,\sigma=\pm 1} (R_{f,\sigma}^+ L_{f,\sigma} + \text{H.c.}) &= 2 \sum_{f,\sigma=\pm 1} \cos[\sqrt{\pi}(\Phi_U + f\Phi_F + \sigma\Phi_c + f\sigma\Phi_{cF})] \\
&= 8\Re e\{e^{i\sqrt{\pi}\Phi_U} [\cos(\sqrt{\pi}\Phi_F) \cos(\sqrt{\pi}\Phi_{cF}) \cos(\sqrt{\pi}\Phi_c) - i \sin(\sqrt{\pi}\Phi_F) \sin(\sqrt{\pi}\Phi_{cF}) \sin(\sqrt{\pi}\Phi_c)]\} \\
&\sim \Re e\{e^{i\sqrt{\pi}\Phi_U} [(\mu_{1F}\mu_{2F}\mu_{3F})(\mu_{3c}\mu_{1c}\mu_{2c}) - i(\sigma_{1F}\sigma_{2F}\sigma_{3F})(\sigma_{3c}\sigma_{1c}\sigma_{2c})]\}.
\end{aligned} \tag{20}$$

In the last line we used the fact that the cosine and sine fields of $\sqrt{\pi}\Phi$ can be expressed in terms of the Ising model order and disorder parameter fields σ and μ , as explained in Appendix A.

Now we can proceed further since the Ising fields can be used to represent the $SU(2)_2$ spin-1/2 primary ones. For example, the spin-1/2 matrix field in the flavor sector can be represented as [48]

$$\begin{aligned}
\hat{G}_{\alpha\beta} &= \hat{I}\sigma_{1F}\sigma_{2F}\sigma_{3F} + i\left(\hat{\tau}^1\mu_{1F}\sigma_{2F}\sigma_{3F} \right. \\
&\quad \left. + \hat{\tau}^2\sigma_{1F}\mu_{2F}\sigma_{3F} + \hat{\tau}^3\sigma_{1F}\sigma_{2F}\mu_{3F}\right),
\end{aligned} \tag{21}$$

where \hat{I} is the identity and $\hat{\tau}^a$ are the Pauli matrices. Since at the critical point the Ising model is self-dual, one can interchange σ_a 's and μ_a 's in Eq. (21) which results in the alternative (dual) representation $\hat{\hat{G}}$. Although correlation functions of \hat{G} and $\hat{\hat{G}}$ are identical, these operators are nonlocal with respect to each other and as such cannot be present in the low-energy action simultaneously.

Looking at Eq. (20), we see that the fermionic bilinears do not factorize into products of single-valued $SU(2)_2$ WZNW fields because they contain mutually nonlocal fields. As we mentioned above, this was noticed already in Ref. [42] for the case of general N_c, N_f . The factorization occurs for conformal blocks, not for single-valued operators. Although the present discussion includes only a particular case, it is intended as an illustration of the general statement, namely, that the projection to the strong coupling vacuum chooses one particular representation. This follows from the fact that the interaction of the color currents

spontaneously breaks the symmetry between the σ and μ vacua such that either σ 's or μ 's condense (they cannot condense together). It is straightforward to check this for the NJL model where the pointlike current-current interaction can be decoupled by the Hubbard-Stratonovich transformation:

$$\frac{g}{2}(\chi_R^a \chi_L^a)^2 \rightarrow \Delta^2/2g + i\Delta(\chi_R^a \chi_L^a). \tag{22}$$

Then one can show that integration over the fermions produces a double-well effective potential for Δ . In the ground state the Z_2 symmetry between the minima is spontaneously broken. Now recall that the Ising model is equivalent to massive Majorana fermion and the sign of the mass determines which of the fields σ or μ condenses. We suggest that the same mechanism works for QCD, which differs from the NJL model only in that the interaction in QCD is long range. The long-range character of the interaction should only strengthen symmetry breaking.

We elaborate further on the projection argument. In the limit of vanishing mass, the eigenstates of our theory are tensor products of the states of the color and the flavor and $U(1)$ sectors. The color and flavor states are created, respectively, by Majorana fermions, Eqs. (18) and (19), and their left-moving counterparts. As we have said, the vacuum in the color sector is double degenerate. In one vacuum, $|0_{c\sigma}\rangle$, we have

$$\langle \sigma_{1c}\sigma_{2c}\sigma_{3c} \rangle \neq 0, \tag{23}$$

while in the other, $|0_{c\mu}\rangle$,

$$\langle \mu_{1c} \mu_{2c} \mu_{3c} \rangle \neq 0, \quad (24)$$

At $T = 0$ the symmetry is spontaneously broken and we have to project the mass term to one of the vacua, say $|0_{c\sigma}\rangle$.

Suppose that vacuum of the theory is $|0_c\rangle$. Let then $|f, 0_{c\sigma}\rangle = f_1^\dagger \cdots f_n^\dagger |0\rangle \otimes |0_{c\sigma}\rangle$, with f^+ being positive momentum components of the flavor Majoranas (19), be a shorthand notation for a flavor excitation above the vacuum. If $\langle 0_{c\sigma} | \sigma_{1c} \sigma_{2c} \sigma_{3c} | 0_{c\sigma} \rangle$ is nonzero then

$$\begin{aligned} \langle f, 0_{c\sigma} | (\mu_{1F} \mu_{2F} \mu_{3F}) (\mu_{3c} \mu_{1c} \mu_{2c}) | f', 0_{c\sigma} \rangle &= 0 \\ \langle f, 0_{c\sigma} | (\sigma_{1F} \sigma_{2F} \sigma_{3F}) (\sigma_{3c} \sigma_{1c} \sigma_{2c}) | f', 0_{c\sigma} \rangle \\ &= \langle 0_{c\sigma} | \sigma_{1c} \sigma_{2c} \sigma_{3c} | 0_{c\sigma} \rangle \langle f | (\sigma_{1F} \sigma_{2F} \sigma_{3F}) | f' \rangle \end{aligned} \quad (25)$$

for states with arbitrary flavor excitations (i.e. $f \neq f' \neq 0$) above the color singlet vacuum. The projection to the color singlet cuts from the mass term the single-valued field \hat{G} acting in the flavor sector with matrix elements between different f and f' . Hence the mass term projected on this ground state is

$$m(R_{f,\sigma}^+ L_{f,\sigma} + \text{H.c.}) \rightarrow \frac{\tilde{m}}{4\pi} (e^{i\sqrt{\pi}\Phi_U} \text{Tr} \hat{G} + \text{H.c.}), \quad (26)$$

where according to (21) $\text{Tr} \hat{G} = 2\sigma_{1F} \sigma_{2F} \sigma_{3F}$ and $\tilde{m} \propto m \langle \sigma_{1c} \sigma_{2c} \sigma_{3c} \rangle$.

The above example illustrates our point that local fields emerge as a result of projection on the singlet ground state of gapped quarks. From this derivation we conjecture that for general N_c and N_f the strong coupling Lagrangian is [41,42]

$$\begin{aligned} \mathcal{L} &= \frac{1}{2} (\partial_\mu \Phi_U)^2 + W[SU(N_f)_{N_c}; G] \\ &+ \frac{\tilde{m}}{4\pi} : (e^{i\sqrt{4\pi/N_c N_f} \Phi_U} \text{Tr} G + \text{H.c.}) : , \end{aligned} \quad (27)$$

where G is the spin-1/2 primary field of the $SU_{N_c}(N_f)$ WZNW model. $: : \text{denotes normal ordering introduced in such a way that the theory has a new ultraviolet cutoff } \Lambda_{\text{QCD}} \sim g$. This means that the two-point correlation function of the operator $\mathcal{O}_{h,\bar{h}}$ with conformal dimensions (h, \bar{h}) is equal to

$$\langle\langle \mathcal{O}(\tau, x) \mathcal{O}(0, 0) \rangle\rangle = [(\tau - ix)]^{-2h} [(\tau + ix)]^{-2\bar{h}}, \quad (28)$$

with \tilde{m} being the renormalized quark mass at the scale of $\Lambda_{\text{QCD}} \sim g$:

$$\tilde{m} \sim m_{\text{ren}} g^{d + \frac{1}{N_c N_f}}, \quad d = \frac{N_c - 1/N_c}{N_c + N_f}, \quad (29)$$

with d being the scaling dimension of the $SU(N_c)_{N_f}$ WZNW matrix field.

III. MATTER AT NONZERO DENSITY

At nonzero chemical potential μ one may shift the $U(1)$ field

$$(4\pi/N_c N_f)^{1/2} \Phi_U \rightarrow 2k_0 x + (4\pi/N_c N_f)^{1/2} \Phi_U. \quad (30)$$

so that $\mu = N_c N_f k_0$. It is expected that the presence of the oscillations makes the mass term irrelevant. In this case we have a ‘‘strange’’ metal: both the charge and flavor excitations are gapless, and all correlation functions of baryons have a power-law decay, with nontrivial scaling exponents. This is true for all values of N_f and N_c for the standard QCD Lagrangian. In Ref. [37], a generalized NJL model was considered possessing a current-current interaction in the $U(1)$ sector. In the presence of such an interaction, a fusion of operators at second order in \tilde{m} may generate quantities where the oscillatory terms cancel and produce a relevant perturbation proportional to $\text{Tr} \Phi_{\text{adj}}$, where Φ_{adj} is a WZNW primary field in the adjoint representation of the flavor symmetry group. This perturbation, in this more generalized setting, gaps out the flavor sector, and the model’s ground state is not a metal. We here however will not consider the addition of this $U(1)$ current-current perturbation to the theory.

In this section we will focus on describing the strange metal that results at nonzero density. This metal has a Luttinger liquid description described by the following effective low-energy bosonic action:

$$\mathcal{L}_{\text{eff}} = \frac{\tilde{K}(\mu)}{2} [v_F(\mu)^{-1} (\partial_t \Phi)^2 + v_F(\mu) (\partial_x \Phi)^2]. \quad (31)$$

This action depends only upon the Luttinger parameter, $\tilde{K}(\mu)$, and the Fermi velocity, $v_F(\mu)$. In the following two subsections, we determine these parameters as a function of μ in two cases. First, for a single flavor, $N_f = 1$, and an arbitrary number of colors, $N_c \geq 2$, where we have recourse to exact methods. Second, in the case of arbitrary flavors and colors, $N_f, N_c \geq 1$, by using perturbative methods appropriate for the case when μ far exceeds the mass gap in the $\mu = 0$ theory. These two parameters determine the low-energy behavior of correlation functions. In the final subsection here we will give an example of this in the specific case of $N_c = 3$ and $N_f = 2$.

A. The case of $N_f = 1$

We begin by determining $\tilde{K}(\mu)$ and $v_F(\mu)$ for $N_f = 1$ as this case allows for an exact treatment in strong coupling. As was discussed in Sec. II A, the resulting low-energy Lagrangian is a sine-Gordon model (15):

$$\mathcal{L} = \frac{1}{2} \left((\partial_\mu \Phi_U)^2 - \frac{\tilde{m}}{2\pi} \cos \left(\sqrt{\frac{4\pi}{N_c}} \Phi_U + 2k_0 x \right) \right). \quad (32)$$

This model is exactly solvable and provides insight into more realistic cases. The spectrum of this model consists of a soliton(s)/antisoliton(\bar{s}) pair and $n = 1, \dots, 2N_c - 2$ breathers. All of these excitations are color singlets. The soliton and antisoliton carry ± 1 $U(1)$ charge and have mass m_s , while the breathers are $U(1)$ neutral and have mass

$$m_n = 2m_s \sin(\pi n \xi / 2), \quad n = 1, \dots, 2N_c - 2 = \nu - 2, \quad (33)$$

with $\xi = 1/(2N_c - 1)$. We first consider what happens to these masses when $\mu > m_s$, answering the fundamental question of what the ground state is of this model at finite density. It turns out that it is metallic, as advertised, consisting of a Fermi sea purely of solitons.

To describe what happens to the spectrum when $\mu > m_s$, we employ the following set of thermodynamic Bethe ansatz (TBA) equations. These equations describe the energies, $\epsilon_{s,\bar{s}}, \epsilon_n$ of the different excitations. These equations, as written below, presume that only the solitons appear in the ground state. If at a given rapidity θ , $\epsilon(\theta) < 0$, the particle appears in the ground state at zero temperature. If $\epsilon(\theta) > 0$ then the particle is excluded from the ground state. The basic idea is that we show these equations are self-consistent, i.e. that if only solitons are supposed to appear in the ground state then we find that $\epsilon_{\bar{s}}, \epsilon_n$ are always positive. The TBA equations are given by [49]

$$\epsilon_s(\theta, \mu) + \int_{-B}^B \mathcal{K}_{ss}(\theta - \theta') \epsilon_s(\theta', \mu) d\theta' = m_s \cosh \theta - \mu, \quad \epsilon_s(B, \mu) = 0; \quad (34)$$

$$\epsilon_{\bar{s}}(\theta, \mu) + \int_{-B}^B \mathcal{K}_{\bar{s}\bar{s}}(\theta - \theta') \epsilon_{\bar{s}}(\theta', \mu) d\theta' = m_s \cosh \theta + \mu; \quad (35)$$

$$\epsilon_n(\theta, \mu) + \int_{-B}^B d\theta' \mathcal{K}_{ns}(\theta - \theta') \epsilon_s(\theta', \mu) = m_n \cosh \theta; \quad (36)$$

$$\mathcal{K}_{ss}(\omega) = \frac{\sinh[(1 - 1/(\nu - 1))\pi\omega/2]}{2 \sinh[\pi\omega/(2(\nu - 1))] \cosh(\pi\omega/2)}; \quad \mathcal{K}_{ns}(\omega) = \frac{\coth[\pi\omega/(2(\nu - 1))] \sinh[\pi n\omega/(2(\nu - 1))]}{\cosh(\pi\omega/2)}. \quad (37)$$

Here $\nu \equiv 2N_c$ and the rapidity θ parametrizes energy-momentum (E/p) of a particle of mass, m , via

$$E = m \cosh(\theta); \quad p = m \sinh(\theta). \quad (38)$$

The parameter B determines the Fermi momentum through $k_F = m_s \sinh(B)$ —see Fig. 8 in Appendix C. Note that k_F is the dressed version of the “bare” Fermi

momentum, k_0 , introduced in (30). More details on the TBA equations are presented in Appendix B. In the above, $\mathcal{K}_{ij}(\omega)$ are the Fourier transforms of $K_{ij}(\theta)$ with respect to θ . The soliton mass can be related to \tilde{m} —see Ref. [50]. When μ exceeds the soliton mass, the soliton spectrum becomes gapless, while the spectral gaps of the antisoliton and the breathers start to increase, as illustrated in Fig. 1 for $N_c = 1$. This demonstrates that it is only the soliton that appears in the ground state and that interactions between the breathers and the Fermi sea of solitons do not lead to the breathers themselves becoming gapless.

Now that we have characterized the finite-density ground state, let us turn to determining the Luttinger parameter, \tilde{K} , and the Fermi velocity v_F . The Luttinger parameter can be extracted [51,52] by solving the equation for the so-called dressed charge, $\zeta(\theta)$:

$$\zeta(\theta) + \int_{-B}^B \mathcal{K}_{ss}(\theta - \theta') \zeta(\theta') d\theta' = 1. \quad (39)$$

The dressed charge measures the change in the charge of the system when one soliton is added to the system while keeping B fixed. The dressed charge is not unity as interactions lead to some of the rapidities of solitons in the Fermi sea exceeding B and so being expelled from the ground state (in the sense of the grand canonical ensemble). The Luttinger parameter is given in terms of the dressed charge as follows:

$$\tilde{K}(\mu) = \zeta^2(B). \quad (40)$$

The numerical analysis of this equation is presented in Appendix C. In the limit of large chemical potential we can however write down the leading-order solution: at $\theta = B$:

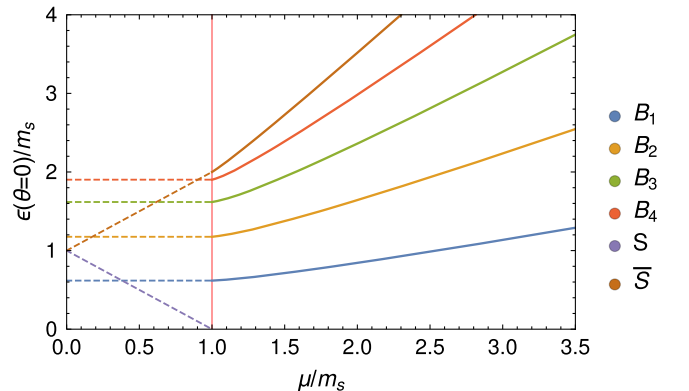


FIG. 1. Spectral gaps of the soliton (S), antisoliton (\bar{S}), and the four breathers, $B_1 \dots B_4$, vs the chemical potential. Here $N_c = 3$, $N_f = 1$, calculated from Eqs. (34)–(37). The spectral gap of the soliton is the mass minus the chemical potential, and vanishes when $\mu = m_s$.

$$\zeta(B) = [1 + \mathcal{K}_{ss}(\omega = 0)]^{-1/2} = (\nu/2)^{-1/2} = N_c^{-1/2}. \quad (41)$$

As the Fermi surface shrinks, so that $B \rightarrow 0$, ζ approaches unity as $\zeta = 1 - 2^{3/2}\mathcal{K}_{ss}(\theta = 0)\delta_\mu^{1/2} + O(\delta_\mu)$ with $\delta_\mu = \mu/m_s - 1$. In fact for any number of flavors, $\tilde{K}(\mu) \rightarrow 1$ as the Fermi surface vanishes, $B \rightarrow 0$.

With the relation $B(\mu)$ in hand, it is then possible to compute the Fermi velocity v_F via

$$v_F = \left. \frac{\partial \epsilon_s(\theta, \mu)}{\partial \theta} \right|_{\theta=B} \frac{1}{2\pi\rho_s(B)}, \quad (42)$$

where the rapidity density distribution function $\rho_s(\theta)$ obeys the same equation as Eq. (34), with the term $m_s \cosh \theta - \mu$ replaced by $(2\pi)^{-1}m_s \cosh \theta$ on the right-hand side. The behavior of the Fermi velocity versus μ is plotted in Fig. 3: it vanishes at threshold, when $\mu = \epsilon_s$, and approaches unity at asymptotically high density.

To summarize, for a single flavor, by projecting onto the color singlet sector, we obtain an effective theory involving only $U(1)$ fields, the sine-Gordon model of Eq. (32). At zero chemical potential, all particles are massive: both the baryons (i.e. solitons and antisolitons) and the mesons (the breathers). At finite density, however, there is an interacting Fermi sea composed solely of baryonic (solitonic) particles. As we show in Sec. III C, this interacting Fermi sea leads to correlation functions characterized by power laws which are a function of the Luttinger parameter, $\tilde{K}(\mu)$.

B. Perturbation theory in the mass

The problem for general N_f and N_c is not integrable. The presence of the mass term changes both the velocity of the $SU(N_f)$ and $U(1)$ excitations as well as the Luttinger parameter \tilde{K} in the $U(1)$ sector. Here we will however focus on the $U(1)$ sector.

At high density, one can compute both \tilde{K} and the velocity of the $U(1)$ excitations, v_F , by expanding in powers of the mass. There are several ways to determine these parameters using perturbation theory. We here focus on computing the charge susceptibility, which is the Fourier transform,

$$\chi(q, \Omega) = \int dx dt e^{iqx + i\Omega t} \chi(x, t), \quad (43)$$

of the two-point function of J_0 , the time component of the $U(1)$ current,

$$\chi(x_1 - x_2, t_1 - t_2) = i\Theta(t_1 - t_2) \langle [J_0(x_1, t_1), J_0(x_2, t_2)] \rangle \quad (44)$$

as given by the usual Kubo formula. It is easy to calculate the susceptibility for imaginary frequencies using the Lehmann spectral expansion, which can be written as a τ -ordered product:

$$\chi(q, \Omega = i\omega) = \int_{-\infty}^{\infty} dx d\tau e^{iqx + i\omega\tau} \times \mathcal{T}_\tau \{ \langle 0 | J_0(x, \tau) J_0(0, 0) | 0 \rangle \}, \quad (45)$$

where $J_0(x, \tau) \equiv J_0(x, t = -i\tau)$.

Let us first recall the exact expression for the $U(1)$ susceptibility in the effective theory Eq. (31). The bosonic field of the effective theory admits the mode expansion

$$\Phi(x, t) = \Phi_0 + L^{-1}\Pi_0 t + \frac{\sqrt{v_F}}{\sqrt{2L\tilde{K}}} \sum_{n \neq 0} \frac{1}{\sqrt{\omega_n}} (a_n e^{ik_n x - i\omega_n t} + a_n^\dagger e^{-ik_n x + i\omega_n t}), \quad (46)$$

where

$$k_n = \frac{2\pi n}{L}, \quad \omega_n = v_F |k_n|. \quad (47)$$

In the effective theory, the $U(1)$ current is given as

$$J_\mu(x, t) = -\frac{\tilde{K}}{\sqrt{\pi}} \epsilon_{\mu\nu} \partial_\nu \Phi(x, t), \quad (48)$$

which ensures that the corresponding charge operator has unit weight on asymptotic states [53]. Differentiating with respect to x_i , performing the sum, and taking the limit $L \rightarrow \infty$, we obtain for the correlator

$$\begin{aligned} & \mathcal{T}_\tau \{ \langle 0 | J_0(x, \tau) J_0(0, 0) | 0 \rangle \} \\ &= -\frac{\tilde{K}}{4\pi^2} \left(\frac{1}{(x + iv_{F0}\tau)^2} + \frac{1}{(x - iv_{F0}\tau)^2} \right). \end{aligned} \quad (49)$$

Straightforward integration then provides the Fourier transform as

$$\chi(q, i\omega) = \frac{v_F \tilde{K}}{\pi} \frac{q^2}{\omega^2 + v_F^2 q^2}. \quad (50)$$

We expect that the above form of the susceptibility holds for strong coupling, low-energy QCD as long as $q \ll 2k_F$. The static susceptibility is given by the subsequent limits $\lim_{q \rightarrow 0} (\lim_{\omega \rightarrow 0} \chi(q, \omega))$:

$$\chi(\omega = q = 0) = \frac{\tilde{K}(\mu)}{\pi v_F(\mu)}. \quad (51)$$

We now turn to computing the same quantity in perturbation theory in \tilde{m} based on the undoped Hamiltonian (27). By comparing the result, we will thus be able to derive an expression for $\tilde{K}(\mu)$ and $v_F(\mu)$ in terms of \tilde{m} .

To proceed, we add a chemical potential to (27) and compute the susceptibility to leading order in \tilde{m}^2 . For small

q , ω , the expansion of the susceptibility is necessarily also an expansion around $\mu = \infty$ and can be written as

$$\chi = \chi_0 + \chi_1 + \dots \quad (52)$$

In the language of the undoped Hamiltonian, the $U(1)$ current, written as J_μ^{undoped} in order to distinguish it from the current operator of the effective theory, is given by

$$J_\mu^{\text{undoped}}(x, t) = -\frac{1}{\sqrt{\pi N_c N_f}} \epsilon_{\mu\nu} \partial_\nu \Phi_U(x, t), \quad (53)$$

where the mode expansion of the field Φ_U has the same structure as Φ in Eq. (46), with the substitutions $v_F \rightarrow 1$, $\tilde{K} \rightarrow 1$.

With the current J^{undoped} , the zeroth-order term of the susceptibility now takes the form

$$\chi(q, i\omega)_0 = \frac{1}{N_c N_f \pi} \frac{q^2}{\omega^2 + q^2}. \quad (54)$$

This form is valid for the system as $\mu \rightarrow \infty$. We thus immediately see

$$\begin{aligned} \tilde{K}(\mu = \infty) &= (N_c N_f)^{-1}; \\ v_F(\mu = \infty) &= 1. \end{aligned} \quad (55)$$

This generalizes our finding from Sec. III A that $\tilde{K}(\mu = \infty) = 1/N_c$ where $N_f = 1$.

Let us now proceed to the first nonvanishing perturbative correction. The Euclidean two-point function is formally written as

$$\begin{aligned} \langle J_0(x_a, \tau_a) J_0(x_b, \tau_b) \rangle_1 &= \frac{1}{2} \left(\frac{\tilde{m}}{4\pi} \right)^2 \frac{1}{\pi N_c N_f} \int_{-\infty}^{\infty} \int_{-\infty}^{\infty} d\tau_1 d\tau_2 \int_{-\infty}^{\infty} \int_{-\infty}^{\infty} dx_1 dx_2 (z_1 - z_2)^{-2\Delta} (\bar{z}_1 - \bar{z}_2)^{-2\Delta} \\ &\quad \times \langle \partial_x \phi(x_a, \tau_a) \partial_x \phi(x_b, \tau_b) (e^{i\beta\phi(x_1, \tau_1)} e^{-i\beta\phi(x_2, \tau_2)} e^{2ik_0(x_1 - x_2)} + e^{-i\beta\phi(x_1, \tau_1)} e^{i\beta\phi(x_2, \tau_2)} e^{-2ik_0(x_1 - x_2)}) \rangle_c, \end{aligned} \quad (60)$$

where $\beta = \sqrt{4\pi/(N_c N_f)}$, $z_{1,2} = \tau_{1,2} - ix_{1,2}$ and the subscript c stands for the connected component of the correlator.

The mass term is a relevant operator for all N_c and N_f . For $N_c = 1$, the dimension is 1 for any N_f as the level 1 WZNW model corresponds to free fermions. When $N_f > 1$, the scaling dimension decreases with increasing N_c and attendantlly the perturbation becomes more relevant. For a fixed N_c , the perturbation becomes less relevant by increasing N_f . Since the perturbation is always strongly

$$\langle J_0(x_a, \tau_a) J_0(x_b, \tau_b) \rangle = \frac{\langle \mathcal{T}_\tau J_0(x_a, \tau_a) J_0(x_b, \tau_b) S \rangle_0}{\langle S \rangle_0}, \quad (56)$$

where

$$\begin{aligned} S &= \sum_{n=0}^{\infty} \frac{(-1)^n}{n!} \int_{-\infty}^{\infty} \dots \int_{-\infty}^{\infty} d\tau_1 \dots d\tau_n \\ &\quad \times \mathcal{T}_\tau \{ V(\tau_1) \dots V(\tau_n) \}, \end{aligned} \quad (57)$$

and V is a shorthand for the mass term in Eq. (27) and \mathcal{T}_τ refers to Euclidean time ordering.

To get the τ -ordered correlator, it is sufficient to compute the expression where the arguments are already in order, $\tau_1 > \tau_2 > \dots > \tau_n$. Analytical continuation in the τ variables then automatically provides the τ -ordered quantity. In the following, we will consider the following normalization of the WZNW two-point function:

$$\langle G_{\alpha_1}^{\beta_1}(z, \bar{z}) G_{\beta_2}^{-1\alpha_2}(0, 0) \rangle = N_f^{-1} \delta_{\alpha_1}^{\alpha_2} \delta_{\beta_1}^{\beta_2} (z\bar{z})^{-2\Delta}, \quad (58)$$

where Δ is the chiral dimension of the $SU_{N_c}(N_f)$ WZNW chiral field G ,

$$\Delta = \frac{N_f^2 - 1}{2N_f(N_c + N_f)}. \quad (59)$$

The normalization is chosen such that the two-point function of $\text{tr } G$ is consistent with (28). Other normalization choices would only affect the relation between \tilde{m} and the bare parameters, the quark mass m and the gauge coupling g . The leading correction reads

relevant for $N_c > 1$, no ultraviolet divergences appear at finite k_0 at second order. The derivation of bosonic expectation values of this type is given in Appendix D. Introducing the parameter

$$\alpha = \left(\frac{\beta^2}{4\pi} + 2\Delta \right) = \frac{1 + N_c N_f}{N_c^2 + N_c N_f}, \quad (61)$$

our calculation gives

$$\begin{aligned} \chi(q, i\omega)_1 = & 2 \left(\frac{\tilde{m}}{4\pi} \right)^2 k_0^{-2+2\alpha} \frac{1}{N_c N_f} \beta^2 \frac{q^2}{(q^2 + \omega^2)^2} \frac{\Gamma(1-\alpha)}{\Gamma(\alpha)} \\ & \times \left\{ -1 + \frac{1}{2} \left[\left(\frac{\omega^2}{(2k_0)^2} + \left(-1 + \frac{q}{2k_0} \right)^2 \right)^{-1+\alpha} + \left(\frac{\omega^2}{(2k_0)^2} + \left(1 + \frac{q}{2k_0} \right)^2 \right)^{-1+\alpha} \right] \right\}. \end{aligned} \quad (62)$$

The Luttinger parameter and the velocity can be obtained separately by a careful examination of the $q \rightarrow 0$, $\omega \rightarrow 0$ limits. First we formally expand the parameters \tilde{K} and v_F in Eq. (50) with respect to a small parameter ϵ :

$$\tilde{K} = \tilde{K}(\mu = \infty) + \epsilon \tilde{K}_1 + \dots \quad (63)$$

$$v_F = v_{F0} + \epsilon v_{F1} + \dots \quad (64)$$

defined as

$$\epsilon = k_0^{-4+2\alpha} \left(\frac{\tilde{m}}{4\pi} \right)^2 \frac{2\pi\beta^2}{4} \frac{\Gamma(1-\alpha)}{\Gamma(\alpha)}. \quad (65)$$

It is convenient to focus our attention on the lines $\omega = \delta q$, δ being a free parameter. In this case Eq. (50) becomes independent of q . Implementing the same substitution to the expansion Eqs. (52)–(54)–(62) and then expanding the resulting expression around $q = 0$, we can directly compare the $O(q^0)$ part of the latter with the effective theory susceptibility Eq. (50). Performing the comparison order by order in δ and solving the resulting system for \tilde{K}_i and v_{Fi} , $i = 0, 1$, we obtain for the first-order corrections

$$\tilde{K}_1 = \tilde{K}(\mu = \infty)(-1 + \alpha)^2, \quad (66)$$

$$v_{F1} = -v_{F0}(-1 + \alpha)(-2 + \alpha). \quad (67)$$

[the zeroth-order terms have already been given in Eq. (55)]. Equations (63)–(67) hold for arbitrary N_c and N_f . In the special case of a single flavor, they can be compared directly to the TBA results, identifying the bare coupling of conformal perturbation theory and using the mass-coupling relation [50]:

$$\begin{aligned} \left(\frac{\tilde{m}}{4\pi} \right)^2 & \rightarrow \mu_{SG}^2 \\ & = \left[m_s \frac{\sqrt{\pi} \Gamma(\frac{1}{2} + \frac{b^2}{2-2b^2})}{2 \Gamma(\frac{b^2}{2-2b^2})} \right]^{4-4b^2} \left(\frac{\Gamma(b^2)}{\pi \Gamma(1-b^2)} \right)^2, \end{aligned} \quad (68)$$

where $b^2 = 1/(2N_c)$. This comparison is given in Fig. 2 for the Luttinger parameter, and in Fig. 3 for the Fermi velocity. The behavior of \tilde{K} for $N_f > 1$ is shown in Fig. 4.

C. Baryonic correlation functions at finite density for $N_c = 3$, $N_f = 2$

In this final part of this section, we write down the elementary correlation functions of some of the baryons for the particular case of $N_c = 3$, $N_f = 2$. The first step is to identify the operators for the baryons. Following the same logic as Ref. [37] these operators involve both the boson ϕ

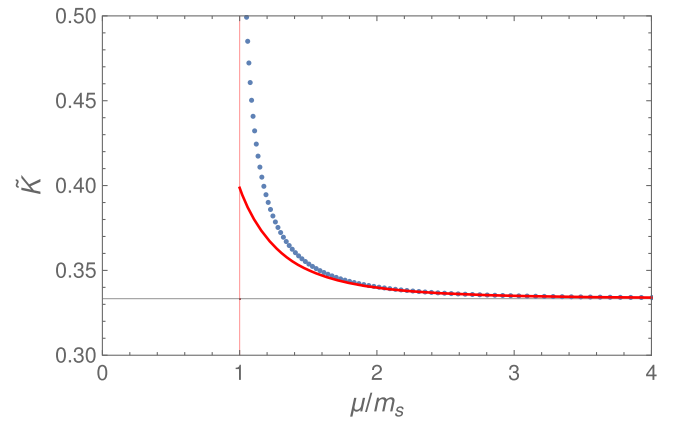


FIG. 2. The Luttinger parameter \tilde{K} as a function of μ , divided by the soliton mass, for the model with $N_f = 1$ and $N_c = 3$. The solid (red) curve is the result to leading order in perturbation theory [Eq. (63)], the dotted (blue) curve from the solution of the thermodynamic Bethe ansatz in Appendix C. The latter shows that this is a Luttinger liquid for any $\mu > m_s$.

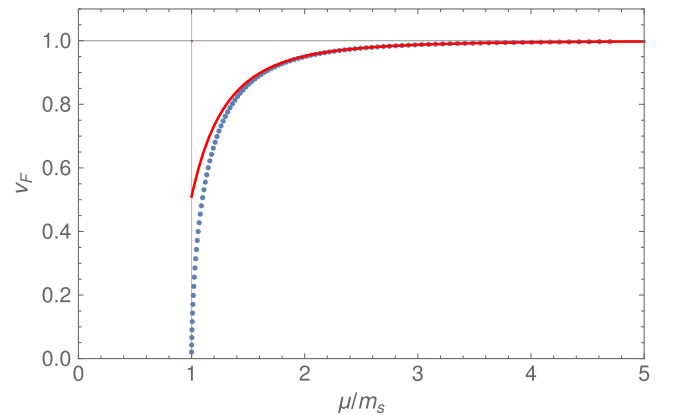


FIG. 3. The Fermi velocity, Eq. (42), vs the chemical potential. The solid (red) curve is the result to leading order in perturbation theory in the mass [Eq. (64)]; the dotted (blue) curve from the solution of the thermodynamic Bethe ansatz in Appendices B and C.

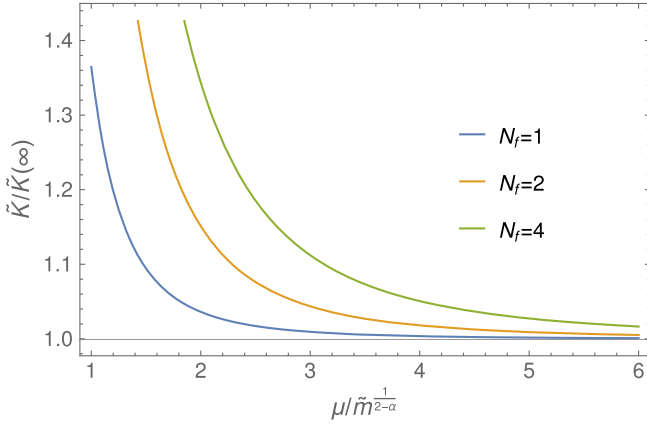


FIG. 4. The relative Luttinger parameter $\bar{K}(\mu)/\bar{K}(\infty)$, $\bar{K}(\infty) = (N_c N_f)^{-1}$ as a function of the dimensionless ratio $\mu/\tilde{m}^{1/(2-\alpha)}$, for the models with $N_c = 3$ and different values of N_f to leading order in perturbation theory (63).

of the low-energy effective Luttinger theory and operators from the $SU(2)_3$ WZNW model. For example, the nucleon of spin-1/2 and the Δ -baryon of spin-3/2 have the following form in the color singlet sector:

$$\begin{aligned} n_R^{\alpha\beta\gamma} &= \epsilon^{abc} R_{a\alpha} R_{b\beta} L_{c\gamma} \sim \\ &\quad \times \exp[i\sqrt{2\pi/3}(2\varphi - \bar{\varphi})] \mathcal{F}_{2/5}^{(1)} \bar{\mathcal{F}}_{3/20}^{(1/2)}, \\ \Delta_R^{\alpha\beta\gamma} &= \epsilon^{abc} R_{a\alpha} R_{b\beta} R_{c\gamma} \sim \exp(3i\sqrt{2\pi/3}\varphi) \mathcal{F}_{3/4}^{(3/2)}. \end{aligned} \quad (69)$$

$$\langle\langle n_R(\tau, x) n_R^\dagger(0, 0) \rangle\rangle = Z_n e^{ik_F x} \left[\frac{(\tau v_F + ix)(\tau v_{f1} + ix)}{(\tau v_F - ix)(\tau v_{f1} - ix)} \right]^{1/4} \left(\frac{\tau_0^2}{\tau^2 + x^2/v_F^2} \right)^{\frac{3}{8} \left(\bar{K} + \frac{1}{9\bar{K}} \right)} \left(\frac{\tau_0^2}{\tau^2 + x^2/v_{f1}^2} \right)^{11/20}, \quad (72)$$

$$\langle\langle \Delta_R(\tau, x) \Delta_R^\dagger(0, 0) \rangle\rangle = Z_\Delta e^{3ik_F x} \left[\frac{(\tau v_F + ix)(\tau v_{f1} + ix)}{(\tau v_F - ix)(\tau v_{f1} - ix)} \right]^{3/4} \left(\frac{\tau_0^2}{\tau^2 + x^2/v_F^2} \right)^{\frac{3}{8} \left(\bar{K} + \frac{1}{\bar{K}} \right)} \left(\frac{\tau_0^2}{\tau^2 + x^2/v_{f1}^2} \right)^{3/4}, \quad (73)$$

where $\tau_0 \sim \epsilon_F^{-1}$, while Z_n and Z_Δ are dimensionful constants depending on ϵ_F . The correlators for the left-moving particles are obtained by replacing $x \rightarrow -x$.

To obtain an idea on how the correlation function appears in frequency-momentum space, we consider the limit $v_F = v_{f1}$. In this limit, the retarded Green's function for the nucleons is

$$\begin{aligned} G_n(\omega, q \pm k_F) &= \frac{Z}{\omega \mp v_F q} \left(\frac{(\omega + i\delta)^2 - v_F^2 q^2}{\epsilon_F^2} \right)^\eta, \\ \eta &= -1/5 + \frac{1}{8} (\sqrt{3\bar{K}} + 1/\sqrt{3\bar{K}})^2, \end{aligned} \quad (74)$$

where δ is an infinitesimal parameter. The general form of the correlation functions of the baryons remains the same

Here \mathcal{F}_h^S are primary fields from the $SU(2)_3$ WZNW model of spin S and scaling dimension h . Both n_R and Δ_R are right moving—their left-moving counterparts are just given by exchanging $R_{a\alpha} \leftrightarrow L_{a\alpha}$. The scaling dimensions of the operators in the $U(1)$ and flavor sector for the nucleon are [37]

$$\begin{aligned} (h, \bar{h})_c &= \left(\frac{1}{48} (3\sqrt{\bar{K}} + 1/\sqrt{\bar{K}})^2, \frac{1}{48} (3\sqrt{\bar{K}} - 1/\sqrt{\bar{K}})^2 \right), \\ (h, \bar{h})_f &= (2/5, 3/20), \end{aligned} \quad (70)$$

while that of the Δ particle is

$$\begin{aligned} (h, \bar{h})_c &= \left(\frac{3}{16} (\sqrt{\bar{K}} + 1/\sqrt{\bar{K}})^2, \frac{3}{16} (\sqrt{\bar{K}} - 1/\sqrt{\bar{K}})^2 \right), \\ (h, \bar{h})_f &= (3/4, 0). \end{aligned} \quad (71)$$

One can see that the scaling dimensions of the fields are determined by the Luttinger parameter, $\bar{K}(\mu)$, of the low-energy bosonic theory.

The correlators for the baryons are like those for Luttinger liquid with spin (i.e. they involve two velocities). For example, the correlators for right-moving baryons are given by (see Eq. (V.9) of Ref. [37]):

for any N_f , but the relation of the scaling dimensions to \bar{K} changes.

We end this section noting that at zero temperature these correlation functions tell us something about instabilities to bosonic condensation in the model. The way this happens depends on the value of the chemical potential. An indicator of the instability is provided by the $T \rightarrow 0$ behavior of the susceptibilities corresponding to the creation of the bosons:

$$\chi = \int_0^{1/T} d\tau \int dx \langle \hat{T} \mathcal{O}(\tau, x) \mathcal{O}(0, 0) \rangle \sim T^{-2+2d_{\mathcal{O}}}, \quad (75)$$

where \mathcal{O} is the field creating a particular type of boson, and $d_{\mathcal{O}}$ is its scaling dimension. In case of the scalar meson,

$d_O = \frac{1}{6\tilde{K}} + 2\Delta$, where Δ was defined in Eq. (59). The condition for the instability to occur is $\tilde{K} \geq 5/21$. In this case we expect that a meson density wave forms. Similarly there is an instability to deuteron superconductivity when $\tilde{K} \leq 7/15$ [37].

We contrast our results here for quarks transforming in the fundamental with that of adjoint quarks considered in Ref. [44]. For adjoint quarks, there are no color singlet fermions; i.e. baryons. For fundamental quarks in $(1+1)d$, there are baryons, but because their Green functions have cuts, not poles, they are incoherent and do not represent well-defined quasiparticles.

IV. FROM 1+1 TO 3+1 DIMENSIONS

In QCD, the behavior of the theory in the limit of low and high density is reasonably well understood.

A. Nuclear matter

At low densities nuclear matter is strongly interacting, but there is no evidence for non-Fermi liquid behavior. For example, the shell model provides an excellent description of nuclei, and there the relevant quasiparticles are certainly nucleons, up to the largest nuclei probed. This is also expected theoretically in infinite nuclear matter: while pions are massless in the chiral limit, they only couple to nucleons through derivative interactions, which do not generate the infrared divergences required for a non-Fermi liquid [54]. Of course there is also superfluidity and superconductivity for dense nucleons, but that is natural in a Fermi liquid in the attractive channels.

B. Perturbative regime

In the opposite limit of high density, by asymptotic freedom perturbation theory in the QCD coupling, g , applies. The dominant effect is the screening of electric gluons through a Debye mass, which cuts off any confinement through the exchange of electric gluons. For quarks near the Fermi surface, there is also a gap due to color superconductivity, but this is exponentially small in $1/\sqrt{g^2}$ [55]. A careful analysis shows that the perturbative regime does exhibit non-Fermi liquid behavior, but for any reasonable range of coupling, the effects are small [56–64].

As an approximate rule of thumb, we can assume that the perturbative regime is entered when the chemical potential, which for on-shell massless quarks is the magnitude of the spatial momentum, is large enough such that perturbative methods can be used. In vacuum, certainly perturbation theory, resummed or not, is not useful below momenta of 1 GeV. Thus the perturbative regime cannot set in before a quark chemical potential of $\mu_{\text{pert}} \approx 1$ GeV. Of course this is a hand-waving argument, and could well be off by a factor of 2. However, heroic computations of the thermodynamic potential to four-loop order, $\sim g^6$, indicate that this is a

reasonable estimate of the quark chemical potential at which the perturbative regime sets in [9–17].

What is not obvious is the behavior of magnetic gluons in the perturbative regime. At nonzero temperature, and zero density, this is an old story [65,66]. At very high temperatures, static electric fields are screened by a Debye mass $m_D \sim \sqrt{g^2}T$. Loop diagrams bring in factors of m_D/T , and so at $T \neq 0$ the perturbative expansion is a power series not in g^2 , but in $\sqrt{g^2}$. This first enters the free energy at $\sim (\sqrt{g^2})^3$.

Since for bosonic fields the timelike component of the (Euclidean) momentum at $T \neq 0$ is an integral multiple of $2\pi T$, we can naturally divide the theory into nonstatic momenta, with $p_0 \sim 2\pi T \neq 0$, and static momenta, with $p_0 = 0$. The fermions can then immediately be dropped, as the timelike component of their (Euclidean) momentum is always an odd multiple of πT . This leaves only the interactions of static magnetic fields without quarks, or a pure $SU(N)$ gauge theory in three dimensions, for which the coupling constant is $g_3^2 = g^2 T$ [67,68]. Since this has dimensions of mass, perturbation theory is an expansion in $g_3^2/p = g^2 T/p$, where p is a characteristic (spatial) momentum of a given diagram. Thus perturbative methods are useless to analyze the infrared limit. Even so, as g_3^2 is the only mass scale in the problem, and as a non-Abelian, superrenormalizable gauge theory, the theory should confine, with a mass gap proportional to the only mass scale in the problem, which is $\sim g_3^2$. This is well confirmed by numerical simulations on the lattice, and enters into the pressure at $\sim g^6$ [69–72].

Now consider the theory at zero temperature and nonzero chemical potential. First, there is no reason to separate out static momenta. As a theory in four dimensions, the timelike component of the momenta, for either boson or fermion fields, is continuous, and can be as small as the spatial momenta. There is Debye screening of electric fields, with a Debye mass $m_D \sim g\mu$. While this causes some delicacy in computing the free energy to high order [9–17], as in the vacuum, at $\mu \neq 0$ perturbation theory remains an expansion in powers of g^2 , and *not* in $\sqrt{g^2}$. Because of the logarithmic infrared divergences in four dimensions, the powers of g^2 are multiplied by powers of logarithms of $\log(m_D^2/\mu^2) \sim \log(g^2)$, but this is very familiar at zero temperature.

The interesting question is then what happens to *magnetic* gluons in cold, dense quark matter? The effective theory has three components. First, there are electric gluons, which are screened by the Debye mass m_D . Second, there are quarks, which (massless or not) develop a small gap about the Fermi surface from color superconductivity. Lastly, there are the magnetic gluons, which by gauge invariance remain massless order by order in perturbation theory. Magnetic gluons do have logarithmic infrared divergences perturbatively, but these are very mild, $\sim g^2 \log(p^2)$ and $\sim g^2 \log(g^2)$. Even so, it

is *inconceivable* that the magnetic fields remain ungapped: as in vacuum, surely over large distances a magnetic mass gap is generated *nonperturbatively*.

The interesting question is then: What is the *ratio* of the mass gap for magnetic gluons to that for electric gluons? The former is nonperturbative, while the latter appears at one-loop order. We assume that in all cases the “masses” are defined in a gauge-invariant manner, such as from the falloff of two-point functions between gauge-invariant operators.

C. Quarkyonic regime

As the quark chemical potential μ increases, we then have the following regimes:

- (i) μ_0 : Where a quark chemical potential first matters, determined kinematically from the condition $\mu_0 = m_B/N_c$, where m_B is the light baryon.
- (ii) $\mu_{\text{Qc}} > \mu > \mu_0$: A strongly interacting Fermi liquid of nucleons.
- (iii) $\mu_{\text{pert}} > \mu > \mu_{\text{Qc}}$: The quarkyonic regime, where the free energy is (approximately) that of (interacting) quarks, but the excitations near the Fermi surface are confined.
- (iv) $\mu > \mu_{\text{pert}}$: The perturbative regime, where electric fields are Debye screened and confinement is lost. Consequently, the value of the Polyakov loop must be near unity. Quarks near the Fermi surface receive a small gap from color superconductivity. It is a non-Fermi liquid, but these effects are mild [56–64]. Magnetic fields are screened nonperturbatively, with the ratio of that mass scale, to the Debye mass, unclear.

We begin by reviewing how the quarkyonic regime can be analyzed by power counting in (fractional) powers of N_c at large N_c [18]. Then we review recent results from numerical simulations on the lattice for two colors [73–95]. By using both methods, we can obtain some guide to the nature of cold, dense QCD, with three colors, and three light flavors.

Given our analysis in 1 + 1 dimensions, one of the central questions is where a non-Fermi liquid emerges. One sign of this is the behavior of the specific heat, which is linear in the temperature as $T \rightarrow 0$, $C(T) \sim T$, but in a non-Fermi liquid, $C(T) \sim T \log(T)$. Of course picking out a logarithm from under a power is always challenging.

Another way to look for the existence of a non-Fermi liquid is to measure the nature of the quark quasiparticles near the putative Fermi surface. In a Fermi liquid, the width of the quasiparticle is much less than the energy, while in a non-Fermi liquid, the width of the quasiparticle is comparable to the energy. Measuring these quantities in a theory with a local gauge symmetry requires developing gauge-invariant probes. The simplest way is to tie two quarks together with a Wilson line [96], and introduce

$$G^{ab}(x, y) = \int \bar{q}_L^{ia}(x) \mathcal{P} \exp \left(ig \int_y^x A_\mu(z) dz \right) q(y)_R^{jb}, \quad (76)$$

where q_L and q_R are left- and right-handed quarks, i and j refer to $SU(N_c)$ color, a and b are flavor indices, and \mathcal{P} is path ordering (with the simplest choice a straight line between x and y).

These quantities are in principle measurable through numerical simulations on the lattice, the functional renormalization group [97], etc.

For three colors, cold, dense QCD can only be studied on the lattice with the quantum computers of the future. This is not true for two colors, where standard Monte Carlo techniques can be used [73–95,98]. However, while the physics of two colors is in some ways very different from that for an odd number of colors, it is still possible to ask *if* a quarkyonic regime arises in the first place.

In all of this we have completely ignored the chiral transition. Unlike the case of zero chemical potential and nonzero temperature, where chiral symmetry restoration occurs well before deconfinement, the situation is reversed at low temperature and large chemical potential. Moving up from the hadronic regime, this is expected to involve the production of a moat regime [35], quantum pion liquids [31,34,99], a critical endpoint [100], and probably many other phenomena, which can be probed experimentally, both in heavy ion collisions at low energy [35], and in neutron stars [31].

1. Large N_c

At least abstractly, the limit of large N_c is especially clean to study [18]. We assume that the number of colors is much larger than the number of flavors, $N_c \gg N_f$, but keep the factors of N_f to understand the generalization to small N_c .

We compare powers of the quark chemical potential μ versus the renormalization mass scale of QCD, which for three flavors is $\Lambda_{\overline{MS}} \sim 340$ MeV. We shall estimate factors of N_c (and N_f) assuming that $\Lambda_{\overline{MS}}$ is about the transition temperature for the restoration of chiral symmetry, which is $T_\chi \approx 154$ MeV. Thus at the outset, our estimates are only good, at best, to a factor of 2. This emphasizes the utility of lattice simulations for two colors in Sec. IV C 2.

At zero chemical potential, in the hadronic phase mesons are weakly interacting, with a pressure of order 1. In the deconfined phase, above a temperature T_d , the pressure is of order $\sim N_c^2$ from gluons, and $\sim N_c N_f$ from quarks. It is natural to expect that the deconfining transition is of first order, with a latent heat $\sim N_c^2$, and this is confirmed by lattice simulations [101,102]. Further, deconfinement is expected to trigger the restoration of chiral symmetry at a temperature T_χ , since for $N_c \gg N_f$ and $\mu = 0$ the dynamics is driven by gluons.

The chemical potential does not matter until $\mu > \mu_0$, when a Fermi sea of baryons can first form. Even though the baryons are strongly interacting, because they are heavy, with a mass $\sim N_c$, the window in which baryons form is narrow, with $\mu_{\text{Qc}} - \mu_0 \sim 1/N_c^2$, Eq. (6) of Ref. [18].

Thus as μ increases from μ_0 , we quickly enter the quarkyonic regime. Consider first chemical potentials which are a number of order 1 times μ_0 . Trivially, the temperature for the deconfining transition, $T_d(\mu) = T_d(0)$, as when $\mu < \mu_0$ a Fermi sphere cannot form. This remains true when μ is a number of order 1 times μ_0 , since the contribution of quarks to the free energy is suppressed by a factor of $\sim N_f/N_c$.

This is not true for the restoration of chiral symmetry. Baryons interact strongly with mesons, and can thereby restore the chiral symmetry. There is another mechanism which is special to $\mu \neq 0$. In nuclear matter, the existence of spatially inhomogeneous condensates is familiar, as pion/kaon condensates [103–106]. For such condensates, a one-dimensional structure forms, and spontaneously breaks both the rotational and flavor symmetries. Although $\langle \bar{q}_L(x)q_R(x) \rangle$ is nonzero locally, it averages to zero as it winds, periodically, along the direction of the condensate. To establish a uniformity of notation, we refer to these as pion/kaon chiral spirals. A pion chiral spiral rotates between, e.g. the σ and π_3 directions, with $\sigma(x)^2 + \pi_3^2(x) = f_\pi^2$. A more complicated kaon chiral spiral, involving all three flavor directions, can also emerge at high density [105,106]. Even at lower densities, though, a kaon chiral kink can develop; for such a condensate, $\langle \bar{s}(x)s(x) \rangle$ is nonzero locally, but again averages to zero along the direction of the kaon chiral kink.

We denote the temperature and chemical potential at which the chiral symmetry is restored as $\mu_\chi(T)$. In contrast to Fig. 1 of Ref. [18], though, it is not necessary that $\mu_\chi(T_d) = \mu_0$, up to corrections of order $\sim 1/N_c^2$, only that $\mu_\chi(T_\chi)$ is within μ_0 by a number of order 1.

In the region where $\mu \sim 1$, although the free energy is quarkyonic, the quasiparticles are uniformly confined. Thus it is appropriate to speak of hadronic chiral spirals, which are best described as a condensate of mesonic fields.

Now let us consider chemical potentials which grow as a fractional power of N_c . To estimate, we assume for the sake of power counting that in the free energy, $T \sim T_\chi$. Then the gluon contribution, $\sim N_c^2 T_\chi^4$, balances the quark contribution, $\sim N_c N_f \mu^4$, when $\mu_{\pi q} \sim (N_c/N_f)^{1/4} T_\chi$. For this range, since the contribution of quarks to the free energy is as large as that of the gluons, we suggest that one goes from a region dominated by hadronic chiral spirals, to one dominated by quark chiral spirals [21,31,33–35,99]. We call them quark, and not quarkyonic, chiral spirals, because both the hadronic and quark chiral spirals occur in the quarkyonic regime.

Thus there are *two* regimes in quarkyonic matter:

- (i) Hadronic (pion/kaon) chiral spirals from $\mu: \mu_{\text{Qc}} \rightarrow \mu_{\pi q} \sim (N_c/N_f)^{1/4} T_\chi$;
- (ii) Quark chiral spirals for $\mu: \mu_{\pi q} \rightarrow \mu_{\text{pert}}$.

This refines previous analysis in Refs. [18,21,33], where the transition between the two types of chiral spirals was not made precise. We stress that there is no phase transition between the region with hadronic chiral spirals and quark chiral spirals; it is just that in each regime, it is more useful to use one description than the other.

To understand what occurs as μ increases further, consider the Debye mass to leading order in perturbation theory:

$$m_D^2 = g^2 \left(\left(N_c + \frac{N_f}{2} \right) \frac{T^2}{3} + N_f \frac{\mu^2}{2\pi^2} \right). \quad (77)$$

When $\mu \sim (N_c/N_f)^{1/2} T_\chi$, the quark contribution to the Debye mass is as large as that of the gluons. This is the perturbative regime, where the screening of electric gluons removes confinement.

It is not evident how to connect this counting powers of N_c/N_f to real scales in QCD. From perturbative computations in QCD [9–17], for three colors perturbation theory is valid for $\mu > \mu_{\text{pert}} \sim 1$ GeV. It is difficult to believe that this scale, μ_{pert} , is very sensitive to either N_c or N_f . In nuclear matter $\mu_0 \sim 300$ MeV. The large N_c expansion predicts that a quarkyonic regime appears at $\mu_{\text{Qc}} = \mu_0 + O(N_f^2/N_c^2)$, that one goes from a regime of hadronic chiral spirals, to one of quark chiral spirals, at $\mu_{\text{H-Qc}} \sim (N_c/N_f)^{1/4} \mu_0$, and lastly, a perturbative regime for $\mu_{\text{pert}} \sim (N_c/N_f)^{1/2} T_\chi$.

How does this apply to QCD, where $N_c = N_f = 3$?

2. Two colors

Because the eigenvalues of the quark determinant are complex for more than two colors, numerical simulations of lattice QCD cannot be carried out with standard Monte Carlo techniques. This is not true for two colors, where the quarks lie in a real representation of the gauge group and the eigenvalues of the quark determinant are real.

Two colors are in some ways rather different from three. Principally, baryons are composed of two quarks, and so are bosons. Thus for two colors, the hadronic regime exhibits Bose-Einstein condensation of the bosonic baryons, instead of a Fermi sea. The behavior about the chemical potential where a Bose-Einstein condensate first forms, $\mu_0 = m_\pi/2$, can be computed in chiral perturbation theory [107–109].

We summarize some results from lattice studies of QC_2D with two flavors. This includes groups from Russia, Refs. [83,84,86,89,92–94,98] and Japan, Refs. [87,90,91,95].

In Ref. [98], $m_\pi \sim 380$ MeV, so $\mu_0 \sim 190$ MeV. For $\mu: 190 \rightarrow 350$ MeV, nuclear matter is a dilute baryon gas, and the value of the diquark condensate agrees with chiral perturbation theory. For higher density, one enters a regime of dense baryons.

In Refs. [84,110], heavier pions were used, with $m_\pi \sim 740$ MeV, and $\mu_0 = 370$ MeV. Chiral perturbation theory is useful to describe the diquark condensate for $\mu: \mu_0 \rightarrow \mu_{\text{QC}}$, where $\mu_{\text{QC}} \sim 540$ MeV; for $\mu > \mu_{\text{QC}}$, the diquark density exceeds the value expected from chiral perturbation theory, computed at lowest order.

The renormalized Polyakov loop is a monotonically increasing function of μ , but even by $\mu \sim 1$ GeV, it is only $\sim 1/3$ its value at the highest μ which was probed, $\mu \sim 2$ GeV. This suggests that $\mu_{\text{pert}} \sim 1$ GeV. This is also confirmed by measurements of the Debye mass, for which m_D/μ is approximately constant from $\mu: 1 \rightarrow 2$ GeV, Figs. 12–14 of Ref. [84]. From Ref. [110], a Fermi sphere forms above $\mu \sim 900$ MeV, with diquarks forming as expected from color superconductivity.

(Incidentally, in Fig. 8 of Ref. [110], the topological susceptibility varies *very* slowly as μ increases, and is still $\approx 75\%$ of its value in vacuum when $\mu = \mu_{\text{pert}}$. See also Fig. 13 of Ref. [87], where qualitatively similar results are found. This agrees with the analysis of Ref. [111]. There, the relative factors of N_c and N_f in the expression for the Debye mass in Eq. (77) suggest that the topological susceptibility varies *much* more slowly with μ than it does with T .)

It is worth contrasting the results for two colors with the qualitative estimates for $N_c = \infty$. First, for two colors, the regime of nuclear matter is rather broad, as $\mu_{\text{QC}} \approx 1.5\mu_0$. Second, as indicated by naive expectation, again μ_{pert} is ≈ 1 GeV. In between lies dense quark matter, which we can hopefully term quarkyonic.

More detailed questions await further study. It is not clear that hadronic chiral spirals will win over Bose-Einstein condensation at low density, or if quark chiral spirals emerge in the quarkyonic phase. Determining the appearance of quark chiral spirals is challenging, as is determining if the quarkyonic regime is a non-Fermi liquid. Both would be useful to study.

One quantity which the lattice has studied is the ratio of the electric to magnetic masses. In Ref. [89], the electric and magnetic propagators were fit to forms suggested by solutions of the Schwinger-Dyson equations. These gauge-variant results find that the electric mass is uniformly heavier than the magnetic. This does not coincide with our expectation that the quarkyonic regime is confining.

Building upon previous analysis in Refs. [87,90,91], however, Ref. [95] studied the profile of the color flux tube. They find that even in high-density superfluid phase, which we term quarkyonic, that the color electric field *is* squeezed into a flux tube, as it is in the hadronic phase, for chemical

potentials as large as $\mu \sim 840$ MeV.¹ This, along with the measurements of the renormalized Polyakov loop, confirms that it is reasonable to assume that electric fields *are* confined in the quarkyonic phase, for $\mu_{\text{QC}} < \mu < \mu_{\text{pert}}$.

Thus simulations for $N_c = N_f = 2$ are essential to demonstrate that the estimates for large N_c , with $N_c \gg N_f$, are a reasonable guide to QCD, where $N_c = N_f = 3$.

D. Quark chiral spirals

To describe quark chiral spirals, we start with the Gribov-Zwanziger form of the electric propagator,

$$\Delta_{00}(p) = \frac{\sigma}{(p^2)^2}. \quad (78)$$

Assuming that we can integrate over the two spatially transverse directions gives a gluon propagator in 1 + 1 dimensions,

$$\int d^2 p_\perp \frac{\sigma}{(p_0^2 + p_z^2 + p_\perp^2)^2} = \frac{\sigma}{p_0^2 + p_z^2}. \quad (79)$$

We shall use this expression to give a qualitative estimate of various quantities below. We note that explicit solutions of the Schwinger-Dyson and functional renormalization group equations find a more complicated form for the gluon propagator [97]. Nevertheless, this expression is useful to give a rough estimate. Assume that one is in the regime of quark chiral spirals, $\mu: \mu_{\pi q} \rightarrow \mu_{\text{pert}}$. Following Refs. [21,33], the confinement scale in 3 + 1 dimensions is proportional to the square root of the string tension, $\sim \sqrt{\sigma}$. If $\mu \gg \sqrt{\sigma} \sim \mu_0$, then it is natural that the Fermi sphere breaks up into a series of patches, with a weak coupling between different patches. The condensate of density waves are described by vectors \mathbf{Q}_a , where the Fermi surface is then covered by these patches, with $a = 1, 2, \dots, \mathcal{N}$. In momentum space at the edge of the Fermi sphere, the area of each patch is $\sim \sigma/v_F$, where v_F is the Fermi velocity. Thus the number of patches is $\mathcal{N} \sim k_F^2/\sigma$.

In the regime of quark chiral spirals, $k_F \sim \mu \geq (N_c/N_f)^{1/4}\mu_0$, and so the number of patches is large, $\mathcal{N} \sim (N_c/N_f)^{1/2}$. The dynamics in a single patch is illustrated in Fig. 5, where for the purposes of illustration we have exaggerated the size of the patch, as the figure only applies to the regime where there are *many* patches, $\mathcal{N} \gg 1$. In Eqs. (11) and (17)–(19) of Ref. [33], the corresponding slow order parameter fields for the density waves are quasi-one-dimensional modifications of those (1 + 1) dimensional QCD, as described in the previous sections. Below we elaborate on the effects of these modifications.

¹E. Itou, private communication.

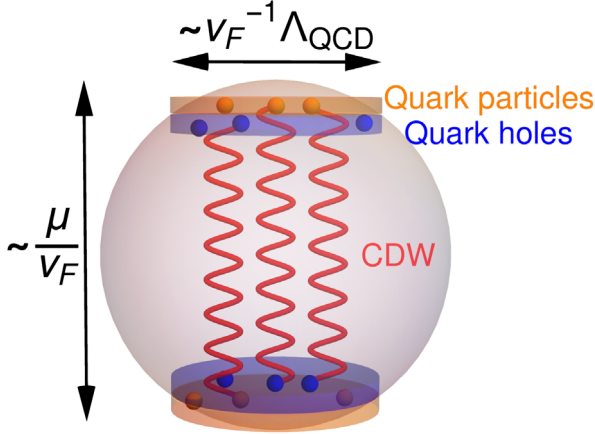


FIG. 5. Due to the singular character of the interaction, quarks at the Fermi surface scatter back and forth inside patches of a particular size.

The case of three pairs of patches is shown in Fig. 6, and illustrates what happens with hadronic (pion/kaon) chiral spirals, in the range $\mu: \mu_{Qc} \rightarrow \mu_{\pi q}$.

Each pair of patches has its own set of fields; a scalar $U(1)$ and a matrix $SU(2N_f)$ field $G_{-\mathbf{Q}} = G_{\mathbf{Q}}^+$. To distinguish them we have to assign to each field a subscript \mathbf{Q} , with the $2N_f$ for an enlarged spin-flavor symmetry. Since wave vectors of the density waves in different patches are not parallel to one another, the direct coupling of the $G_{\mathbf{Q}}$ complex matrix fields with different \mathbf{Q} is suppressed, at

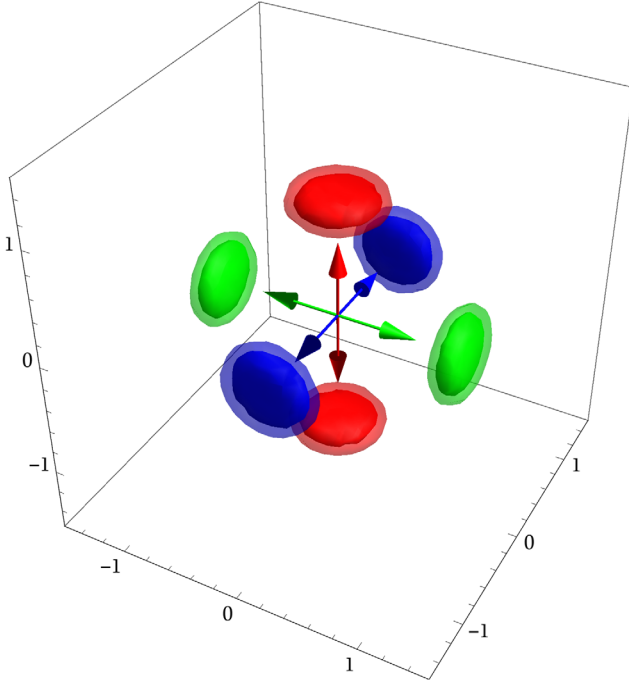


FIG. 6. The contour plots of the meson spectrum Eq. (81) for the smallest possible number of patches, six, for a cubic arrangement of density waves. We set $\alpha = 1$, with the axes wave vectors $q_{x,y,z}/2k_F$.

least at large \mathcal{N} . However, inside a given patch the excitations have a transverse dispersion which makes the $(3+1)$ -dimensional case somewhat different from that in $(1+1)$ dimensions. The energies of the meson fields depend upon the momenta transverse to the wave vector of their patch \mathbf{Q}_a , where $|\mathbf{Q}_a| \approx 2k_F$. As for smectic liquid crystals, the stiffness in the direction transverse to \mathbf{Q} vanishes, and the dispersion relation is anisotropic. The action for each pair is the $U(1) \times SU_{N_c}(2N_f)$ WZNW model, augmented by a term which depends upon the transverse momenta:

$$-\frac{\alpha v_F}{(2k_F)^4} \text{Tr}(G_{\mathbf{Q}}^+[\mathbf{Q} \times \nabla]^2 G_{\mathbf{Q}})^2, \quad (80)$$

where α is a numerical coefficient. Linearizing the fluctuations of G , the mesonic modes have the dispersion relation

$$\omega_{\mathbf{Q}}(\mathbf{q})^2 = (v_F/2k_F)^2 \{[\mathbf{Q} \cdot (\mathbf{q} - \mathbf{Q})]^2 + \alpha[(\mathbf{Q} \times \mathbf{q})^2]/4k_F^2\}. \quad (81)$$

The transverse fluctuations introduce a new energy scale, as the width of the fluctuations in the transverse direction, $W \sim \sigma/k_F \sim k_F/\mathcal{N}$. This scale marks a crossover from the $(1+1)d$ -dimensional regime to one where transverse fluctuations are important. The separation of $U(1)$ charge and spin-flavor holds above the crossover scale W , where the composite description of Eq. (69) apply. The baryons are incoherent for energies above W , and coherent for those below. Below W , the transverse fluctuations enter, and one cannot directly apply the bosonization formulas to calculate baryon correlation functions. A reasonable assumption is that since the spectrum of the fundamental excitations, which are mesons, is gapped everywhere except at the discrete set of points in momentum space, the baryons lack an extended Fermi surface.

The vanishing of the Fermi surface affects the thermodynamics for temperatures $T \sim W$. At temperatures above $\sim W$ the system is a Luttinger liquid, with the specific heat linear in temperature $\sim T/\epsilon_F$.

At temperatures below $\sim W$, the specific heat is $\sim T^2(\mathcal{N}/\epsilon_F)$. To get a more detailed description of the crossover we treat the size of the patch as a rigid cutoff for the transverse momentum, and normalize behavior for $T \gg W$ to the asymptotic form for the specific heat for a conformal field theory. In this case, it is for a $U(1) \times SU_{N_c}(2N_f)$ WZNW model, where the central charge is $C = 1 + N_c(4N_F^2 - 1)/(2N_f + N_c)$. Then the temperature dependence of the specific heat is given by the formula

$$C_v/T = 2k_F^3 C \gamma(T/W; \alpha),$$

$$\gamma(t, \alpha) = t \int_0^\infty dx \int_0^{1/t} dy \frac{(x^2 + \alpha y^2)}{\sinh(\sqrt{x^2 + \alpha y^2}/2)}, \quad (82)$$

where the function $\gamma(t, 1)$ is depicted in Fig. 7.

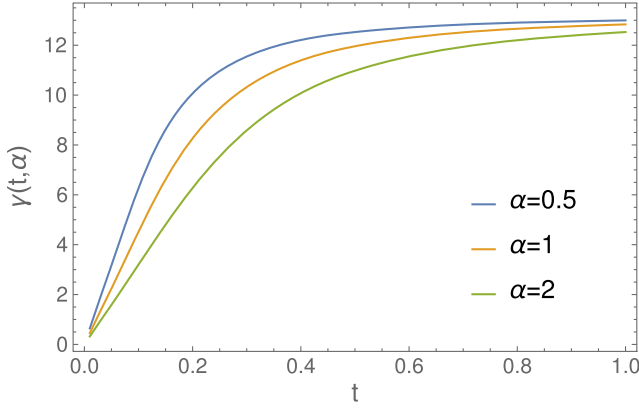


FIG. 7. The specific heat divided by temperature, $\gamma(t, \alpha)$ in Eq. (82), for $\alpha = 0, 5, 1, 2$, as a function of $t = T/W$.

The softness of the transverse dispersion strengthens the thermal fluctuations preventing the development of any kind of long-range order at finite temperature. The non-Fermi liquid is a critical state and is incompatible with long-range order. Formally the destruction of the long-range order is related to the divergence of the integral,

$$T \sum_n \int \frac{dq_{\parallel} d^2 q_{\perp}}{(2\pi T n)^2 + \omega^2(q)} = \int \frac{dq_{\parallel} d^2 q_{\perp}}{2\omega(q)} \coth[\omega(q)/2T],$$

measuring the relative fluctuations of the order parameter fields. This integral converges at $T = 0$ and logarithmically diverges at nonzero temperature when it is dominated by the $n = 0$ Matsubara frequency:

$$T \int \frac{dq_{\parallel} d^2 q_{\perp}}{q_{\parallel}^2 + \alpha q_{\perp}^4 / 4k_F^2}. \quad (83)$$

In Ref. [33] we argued that at finite T the Abelian sector of the theory remains critical with temperature-dependent power-law correlations, but the non-Abelian flavor fluctuations acquire a correlation length exponentially large in $1/T$. This difference is related to the fact that the low-energy theory for the Abelian sector is Gaussian, but the non-Abelian sector is described by the nonlinear sigma model where the interactions generate a finite correlation length.

We comment that if the condensate arises from a moat spectrum, then the correlation lengths of the non-Abelian fields remain finite at zero temperature [31]. This correlation length is exponentially large in the coupling constant, and implicitly we assume that this correlation length is larger than all scales above. Even if this scale is commensurate with those above, the results do not change qualitatively.

E. Neutrino emission

Most properties of cold quark matter are difficult to observe directly. Because neutron stars are transparent to

neutrinos, neutrino emission can be inferred, albeit indirectly, by the cooling of neutron stars [112–118].

In pion/kaon condensates, it is known that effective quasiparticles enhance neutrino emission, through their decay into a quasiparticle neutron-proton pair [112–117]. As discussed in the previous section, there are strong similarities between pion/kaon condensates and the condensates in the quarkyonic phase.

Thus it is natural to expect that neutrino emission is similarly enhanced in the quarkyonic phase [36]. Fluctuations of the WZNW matrix fields decay into a virtual nucleon pair, and thereby through the weak interaction into a lepton neutrino pair [119]:

$$\begin{aligned} \mathcal{L}_W \sim ig_W \sum_{\mathbf{Q}} [\bar{e}(\mathbf{Q} \cdot \boldsymbol{\gamma})(1 - \gamma_5)v_e + \bar{\mu}(\mathbf{Q} \cdot \boldsymbol{\gamma})(1 - \gamma_5)v_{\mu}] \\ \times (\text{Tr}(G^+ \mathbf{Q} \cdot \nabla G \hat{\tau}^+)) + \text{H.c.}, \end{aligned} \quad (84)$$

where G is the $SU(2)$ flavor WZNW matrix field for a given patch vector \mathbf{Q} , $\boldsymbol{\gamma}$ are Dirac gamma matrices with spacelike indices, and $\hat{\tau}^+$ is the Pauli matrix acting on flavor indices of G [33] (we dropped the subscript \mathbf{Q}).

The neutrino emissivity is

$$\mathcal{E}_{\nu} = 2 \int \frac{d^3 p_{\nu}}{(2\pi)^3} p_{\nu} \frac{\partial}{\partial t} f_{\nu}(t, \mathbf{p}), \quad (85)$$

where f_{ν} is the neutrino distribution function. Following Ref. [118],

$$\mathcal{E}_{\nu} \sim \mu_e \rho(\epsilon_F) T^6 g_s^2(T), \quad (86)$$

where μ_e is the chemical potential of the electrons, $\rho(\epsilon_F)$ is the quark density of states and $g_s(T)$ is the running coupling constant. Since $\rho(\epsilon_F)$ is proportional to the specific heat, we can write

$$\mathcal{E}_{\nu} \sim \mu_e \left(\frac{\partial S}{\partial T} \right) T^6 g_s^2(T), \quad (87)$$

where S is the entropy. Substituting this into the equation $\frac{\partial F}{\partial t} = -\mathcal{E}_{\nu}(T)$, where F is the free energy per unit volume, we obtain the equation for the temperature as a function of time:

$$\frac{\partial T}{\partial t} = -A \mu_e \left(\frac{\partial \ln S}{\partial T} \right) T^6 g_s^2(T), \quad (88)$$

where A is a temperature-independent proportionality coefficient.

For $\epsilon_F > T > W \sim \epsilon_F/\mathcal{N}$, the density of states is constant, while at lower temperatures we replace $\rho(\epsilon_F)$ by T/W . The right-hand side of Eq. (88) contains $\ln S \sim n \ln T$, where $n = 1$ for $T \gg W$ and $n = 2$ for $T \ll W$. The temperature dependence of the strong coupling constant $g_s(T)$ can be neglected, as that is only logarithmic. So approximately,

$$T = \frac{T_0}{(1 + t/\tau)^{1/4}}, \quad 1/\tau \sim nT_0^4 g^2(T_0) \mu_e. \quad (89)$$

where T_0 is the temperature at time $t = 0$. The same time dependence is found with weakly interacting quarks, the only difference being the overall numerical coefficient in front. This difference, however, is important, and it would be well worth studying in detail.

V. CONCLUSIONS

In this paper we considered the strange-metal phase of QCD in $(1+1)$ dimensions, and explored the consequences for quarkyonic matter in $(3+1)$ dimensions. In $1+1$ dimensions a strange metal exists above a given quark density; it is a critical phase, where nucleon excitations are incoherent and essentially a Tomonaga-Luttinger liquid. In $(3+1)$ dimensions the low-energy theory remains very similar, as it remains a nonlinear sigma model for the collective mesonic modes, with the baryons topological excitations of the meson field. The spectrum of the mesons is highly anisotropic, and is very soft in the direction tangential to the Fermi surface. This introduces an extra energy scale related to the crossover from the regime of one-dimensional fluctuations at high energy, to the regime of anisotropic three-dimensional fluctuations at low energies. Above this energy scale the Luttinger liquid description of the quarkyonic state remains valid and the nucleons are incoherent. We have not been able to determine whether fermionic quasiparticles exist at lowest energies. We also explored the consequences for neutrino emission from neutron stars.

ACKNOWLEDGMENTS

M. L., A. M. T., and R. M. K. are supported by Office of Basic Energy Sciences, Material Sciences and Engineering Division, U.S. Department of Energy (DOE) under Contract No. DE-SC0012704. R. D. P. was supported by the U.S. DOE under Contract No. DE-SC001270, by B. N. L. under the Lab Directed Research and Development program 18-036, and by the U.S. DOE, Office of Science, National Quantum Information Science Research Centers, Co-design Center for Quantum Advantage (C2QA) under Contract No. DE-SC001270. We thank Toru Kojo for allowing us to use a figure of his, which we modified into our Fig. 5. R. D. P. also thanks Vitaly Boryakov, Victor Braguta, Etsuko Itou, and Roman Rogalyov for helpful discussions of their work.

APPENDIX A: FACTS ABOUT QUANTUM ISING MODEL

The quantum Ising model on a lattice is defined as

$$H = -\sum_n (J\sigma_n^x \sigma_{n+1}^x - h\sigma_n^z), \quad (A1)$$

where σ^a are the Pauli matrices. It allows a self-dual representation in terms of other Pauli matrix operators defined on the dual lattice,

$$\mu_{n+1/2}^z = \sigma_n^x \sigma_{n+1}^x, \quad \mu_{n+1/2}^x = \prod_{j=1}^n \sigma_j^z, \quad (A2)$$

so that

$$H = -\sum_n (J\mu_{n+1/2}^z - h\mu_{n+1/2}^x \mu_{n-1/2}^x). \quad (A3)$$

It is obvious that at $J \gg h$ the ground state of (A1) is such that $\langle \sigma^x \rangle \neq 0$ and at $J \ll h$ the ground state of (A2) is such that $\langle \mu^x \rangle \neq 0$. Since σ^x and μ^x cannot order simultaneously, we conclude that the point $J = h$ is critical separating two phases of model (A1).

Using the Jordan-Wigner transformation, one can transform (A1) into a Hamiltonian of noninteracting Majorana fermions ρ_n, η_n with anticommutation relations

$$\{\rho_n, \rho_m\} = \{\eta_n, \eta_m\} = \delta_{nm}, \quad \{\rho_n, \eta_m\} = 0, \quad (A4)$$

i.e.

$$H = i \sum_n (J\rho_n \eta_{n+1} - h\rho_n \eta_n). \quad (A5)$$

As far as applications to quantum field theory are concerned, we need to pass to the continuum limit via defining $n = x/a_0$ with $a_0 \rightarrow 0$ the lattice spacing or, alternatively, momentum cutoff. The continuum limit of σ^x and μ^x operators become the order and disorder fields $\sigma(x)$ and $\mu(x)$. The continuum limit of the Majoranas is related to the chiral fields used in the main text as

$$\frac{1}{a_0} \rho_n \rightarrow \chi_R + \chi_L, \quad \frac{1}{a_0} \eta_n \rightarrow \chi_R - \chi_L. \quad (A6)$$

At the critical point, $J = h$, the fields σ, μ are primary fields with conformal dimensions $(1/16, 1/16)$. The right- and left-moving Majorana fields have conformal dimensions $(1/2, 0)$ and $(0, 1/2)$, respectively.

Since two species of real Majorana fermions form a complex Dirac fermion which in turn can be bosonized and described by the Gaussian model of a bosonic field Φ , one can establish a correspondence between σ, μ and the bosonic field. This correspondence was first given by Itzykson and Zuber as [120]

$$\begin{aligned} \mu_1 \mu_2 &\sim \cos(\sqrt{\pi}\Phi), & \sigma_1 \sigma_2 &\sim \sin(\sqrt{\pi}\Phi), \\ \sigma_1 \mu_2 &\sim \cos(\sqrt{\pi}\Theta), & \mu_1 \sigma_2 &\sim \sin(\sqrt{\pi}\Theta), \end{aligned} \quad (A7)$$

where $\Theta = \varphi - \bar{\varphi}$ is a field dual to Φ . These are the identities that we use in the main text.

As is shown in the main text, the color and flavor sectors in the model with $N_c = N_f = 2$ are described by six Majorana fermions which naturally split into two groups of three. The interaction of the color currents includes three Majorana fermions corresponding to three critical Ising models. The interaction leads to a spontaneous breaking of the $[Z_2]^3$ symmetry in the color sector generating vacuum averages either for μ or σ fields of the corresponding Ising models.

APPENDIX B: THERMODYNAMIC BETHE ANSATZ

In the sine-Gordon theory, on-shell scattering is purely elastic (in the sense that the number of particles and the set of rapidities always has to be the same in the in and out state) and it factorizes completely. Knowledge of the $2 \rightarrow 2$ elastic scattering phases between all particle types provides a complete description of all scattering processes. This makes it an integrable model. At a general sine-Gordon coupling, scattering is not completely diagonal due to the possibility of $s\bar{s} \rightarrow \bar{s}s$ scattering. In our cases of interest ($N_c \in \mathbb{Z}$) these off-diagonal amplitudes are exactly zero, which simplifies the discussion.

To derive the thermodynamics, it is useful to adopt a first quantized viewpoint, where a state is described by a multiparticle wave function. For a moment let us restrict the model onto a circle of circumference L . Since it is a relativistic system, interactions are local. Particles propagate freely between pointlike interactions, when they acquire a phase determined by the S -matrix element. This provides the quantization condition for the particles up to exponentially small corrections for large L :

$$e^{ip_j L} \prod_{k \neq j} S_{r_j r_k}(\theta_j - \theta_k) = 1, \quad (\text{B1})$$

where r_i specifies the type of particle i . Taking the logarithm, one has

$$m_{r_j} L \sinh \theta_j + \sum_{k \neq j} \delta_{r_j r_k}(\theta_j - \theta_k) = 2\pi n_j, \quad n_j \in \mathbb{Z}, \quad (\text{B2})$$

where

$$\delta_{r_j r_k}(\theta) = -i \log S_{r_j r_k}(\theta). \quad (\text{B3})$$

The set of equations (B2) is commonly referred to as the asymptotic Bethe ansatz or Bethe-Yang equations. The energy and momentum of multiparticle states are simply given as a sum of one-particle states with the obtained rapidities

$$E = \sum_j m_{r_j} \cosh \theta_j, \quad P = \sum_j m_{r_j} \sinh \theta_j. \quad (\text{B4})$$

In the sine-Gordon model these S -matrix elements are well known. They have the form ($N_c \in \mathbb{Z}$)

$$S_{ss}(\theta) = S_{s\bar{s}}(\theta) = S_{\bar{s}s}(\theta) = S_{\bar{s}\bar{s}}(\theta) \quad (\text{B5})$$

$$= -e^{\int_0^\infty dt \frac{\sinh(\nu-2)t}{t \sinh(t) \cosh((\nu-1)t)} \sinh\left(\frac{2t\theta(\nu-1)}{\pi}\right)}, \quad (\text{B6})$$

$$S_{sn}(\theta) = S_{ns}(\theta) = S_{\bar{s}n}(\theta) = S_{n\bar{s}}(\theta) \quad (\text{B7})$$

$$= \frac{\sinh \theta + i \cos \frac{n\pi}{2(\nu-1)} \prod_{k=1}^{n-1} \sin^2\left(\frac{n-2k}{4(\nu-1)} \pi - \frac{\pi}{4} + i \frac{\theta}{2}\right)}{\sinh \theta - i \cos \frac{n\pi}{2(\nu-1)} \prod_{k=1}^{n-1} \sin^2\left(\frac{n-2k}{4(\nu-1)} \pi - \frac{\pi}{4} - i \frac{\theta}{2}\right)}. \quad (\text{B8})$$

We now focus on the case of finite soliton density. In the ground state of our setup, all soliton states are filled up to a threshold rapidity B , and none above. To obtain the continuum limit of the quantization condition, we introduce the rapidity density $\rho_s(\theta)$. Denoting the total number of *soliton* one-particle states between rapidity 0 and θ with $N(\theta)$, the rapidity density is defined as $\rho_s(\theta) = L^{-1} \frac{dN}{d\theta}$.

Therefore, $n_j = L \int_0^{\theta_j} \rho_s(\theta') d\theta'$.

Let us first consider the finite-density ground state. The sum in Eq. (B2) can be rewritten as an integral over rapidities (dropping the index j)

$$\begin{aligned} m_s L \sinh \theta + L \int_{-B}^B d\theta' \rho_s(\theta') \delta_{ss}(\theta - \theta') \\ = 2\pi L \int_0^\theta \rho_s(\theta') d\theta'. \end{aligned} \quad (\text{B9})$$

Differentiating with respect to θ , we obtain an integral equation for $\rho_s(\theta)$,

$$\frac{m_s}{2\pi} \cosh \theta = \rho_s(\theta) + \int_{-B}^B d\theta' \rho_s(\theta') \mathcal{K}_{ss}(\theta - \theta'), \quad (\text{B10})$$

where $\mathcal{K}_{ss}(\theta) = -\frac{1}{2\pi} \partial_\theta \delta_{ss}(\theta)$. The solution can be written formally as

$$\rho_s(\theta) = (1 - \mathcal{K}_{ss})^{-1} \left[\frac{m_s}{2\pi} \cosh \theta \right]. \quad (\text{B11})$$

The energy of the finite- B ground state is thus

$$E_0 = \sum_j m_s \cosh \theta_j = L \int_{-B}^B \rho_s(\theta) (m_s \cosh \theta - \mu) d\theta. \quad (\text{B12})$$

The operator $(1 - \mathcal{K}_{ss})^{-1}$ is symmetric, so the ground-state energy is equivalently written as

$$E_0 = L m_s \int_{-B}^B \frac{d\theta}{2\pi} \cosh \theta \cdot \epsilon_s(\theta), \quad (\text{B13})$$

where the soliton spectral gap $\epsilon_s(\theta)$ is the solution of the Fredholm equation with inhomogeneity $m_s \cosh \theta - \mu$,

$$\epsilon_s(\theta) = (1 - \mathcal{K}_{ss})^{-1} [m_s \cosh \theta - \mu], \quad (\text{B14})$$

and the total $U(1)$ charge is the number of solitons in the condensate,

$$Q_0 = L \int_{-B}^B \rho_s(\theta) d\theta = L m_s \int_{-B}^B \frac{d\theta}{2\pi} \cosh \theta \cdot \zeta(\theta) \quad (\text{B15})$$

where $\zeta(\theta) = (1 - \mathcal{K}_{ss})^{-1} [1]$ is the dressed charge in Eq. (39).

Consider now adding an extra particle of type r with rapidity θ_0 to the condensate. The modified quantization condition to the condensate reads

$$2\pi n_j = m_s L \sinh \theta_j + \delta_{rs}(\theta_j - \theta_0) + \sum_{k \neq j} \delta_{ss}(\theta_j - \theta_k),$$

$$n_j \in \mathbb{Z}. \quad (\text{B16})$$

In the continuum,

$$\frac{m_s}{2\pi} \cosh \theta = \tilde{\rho}(\theta) + \int_{-B}^B d\theta' \tilde{\rho}(\theta') \mathcal{K}_{ss}(\theta - \theta') - \frac{1}{2\pi L} \partial_\theta \delta_{rs}(\theta - \theta_0). \quad (\text{B17})$$

The equation for the density difference with respect to the ground state $D_{\theta_0}(\theta) = L[\tilde{\rho}(\theta) - \rho_s(\theta)]$ takes the form

$$D_{\theta_0}(\theta) = (1 - \mathcal{K}_{ss})^{-1} [-\mathcal{K}_{rs}(\theta - \theta_0)], \quad (\text{B18})$$

with $\mathcal{K}_{rs}(\theta - \theta_0) = -\frac{1}{2\pi} \partial_\theta \delta_{rs}(\theta - \theta_0)$. The energy difference due to the extra particle is then

$$E_1 - E_0 \equiv \epsilon_r(\theta_0)$$

$$= m_r \cosh \theta_0 - \mu Q_r + \int_{-B}^B D_{\theta_0}(\theta) [m_s \cosh \theta - \mu] d\theta$$

$$= m_r \cosh \theta_0 - \mu Q_r - \int_{-B}^B \mathcal{K}_{rs}(\theta - \theta_0) \epsilon_s(\theta) d\theta, \quad (\text{B19})$$

in agreement with Eqs. (34)–(35). Here $Q_s = +1$, $Q_{\bar{s}} = -1$ and $Q_r = 0$ otherwise. When $r = s$, this yields the Fredholm equation for ϵ_s . For $r \neq s$, the spectral gap can be calculated straightforwardly once ϵ_s is known. When an extra soliton of rapidity θ_0 is added to the system, the net extra charge

$$Q_1 - Q_0 = 1 + \int_{-B}^B D_{\theta_0}(\theta) d\theta \quad (\text{B20})$$

$$= 1 - \int_{-B}^B \mathcal{K}_{ss}(\theta - \theta_0) \zeta(\theta) \equiv \zeta(\theta_0) \quad (\text{B21})$$

equals $\zeta(\theta_0)$. Hence the name “dressed charge.”

APPENDIX C: NUMERICAL ANALYSIS FOR A SINGLE FLAVOR

The integral equations (34)–(39) can be solved independently. They are all Fredholm equations of the second kind, for which many numerical methods exist. In fact TBA equations of this type can be solved well beyond machine precision (see e.g. [121]). A simple yet efficient method is provided by the Nystrom method [122]. In case of an integer number of colors N_c , the kernel function $K(\theta)$ can be written in a closed form in terms of digamma functions:

$$\mathcal{K}(\theta) = -\frac{1}{2\pi} \frac{d\delta(\theta)}{d\theta} = \frac{1}{4\pi^2} \sum_{n=0}^{\nu-2} \left[\psi \left(\frac{1}{2} \left(1 - \frac{i\theta}{\pi} + \frac{n}{\nu-1} \right) \right) + \psi \left(\frac{1}{2} \left(1 + \frac{i\theta}{\pi} + \frac{n}{\nu-1} \right) \right) - \psi \left(\frac{\pi + n\pi - i\theta(\nu-1)}{2\pi(\nu-1)} \right) - \psi \left(\frac{\pi + n\pi + i\theta(\nu-1)}{2\pi(\nu-1)} \right) \right]. \quad (\text{C1})$$

By a change of variables $\theta = By$, $\theta' = By'$, $\hat{\epsilon}(y) = \epsilon(By)$, $\hat{G}(y, y') = \mathcal{K}(B(y - y'))$, we transform the integral equations to the interval $[-1, 1]$. For example, Eq. (34) takes the form

$$\hat{\epsilon}(y) + B \int_{-1}^1 dy' \hat{G}(y, y') \hat{\epsilon}(y') = m_s \cosh(By) - \mu, \quad (\text{C2})$$

and the boundary condition becomes $\hat{\epsilon}(\pm 1) = 0$.

The integral in Eq. (C2) is then approximated by the Gauss-Legendre quadrature rule. This means that the integrand is to be evaluated at the roots y_i , $i \in 1, \dots, N$ of the N th Legendre polynomial. To this end, we introduce N -component vectors $\hat{\epsilon}_i \equiv \hat{\epsilon}(y_i)$, $u_i = m_s \cosh(By_i) - \mu$ and the matrix $\hat{G}_{ij} = \hat{G}(y_i, y_j)$. The components of the vector $\hat{\epsilon}(y_i)$ are obtained through the solution of the linear system

$$(1_{ij} + Bw_j \hat{G}_{ij}) \hat{\epsilon}_j = u_i, \quad (\text{C3})$$

where w_j are the quadrature weights. Finally, the solution is given by substituting back to Eq. (C2) and using the quadrature rule

$$\hat{\epsilon}(y) \approx m_s \cosh(By) - \mu - B \sum_{i=1}^N w_i \hat{G}(y, y_i) \hat{\epsilon}_i. \quad (\text{C4})$$

This provides a robust way to reproduce the unknown function and its derivative.

The results for $\zeta(\theta)$ are shown in Fig. 8(a). Note the plateau that develops for large values of B . Equation (39)

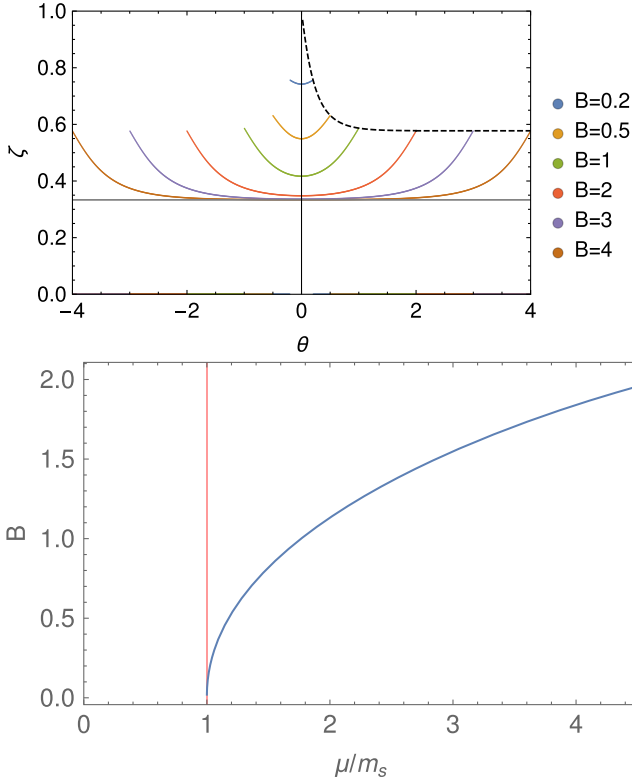


FIG. 8. Numerical solution of the TBA equations [(34)–(39)] for $N_c = 3$, $m_s = 1$. On the top panel, solutions for different B values are shown. The $\zeta - B$ relation is drawn with a dashed curve ($\zeta = \sqrt{K}$ is the dressed charge). On the bottom, the relation $B(\mu)$ is shown.

has a constant bulk solution as $B \rightarrow \infty$, which can be obtained by a simple Fourier transform. Also plotted are the asymptotic values $\zeta_{\text{bulk}} = 2/\nu$. This signals that the $B \rightarrow \infty$ limit has to be taken carefully as the behavior at the boundary is never reproduced from the bulk solution.

It is easy to obtain the (inverse) relation $\mu(B)$ from Eq. (34). A simple implementation of the secant method, connected to the Fredholm solver for $\epsilon(B, \mu)$, converges to the root $\epsilon(\mu) = 0$ within a small number of iterations for each point. The result is depicted in Fig. 8(b). The $\zeta - \mu$ relation is plotted in Fig. 2. There is a phase transition at $\mu = m_s (= 1)$. The parameter ζ approaches 1 in this limit. Increasing μ , ζ quickly takes its asymptotic value, $\zeta_* = \sqrt{2/\nu}$.

We note that the relation $\mu(B)$ is available analytically through a large- B expansion, which is provided in implicit form in [50]. This was useful to check the accuracy of the numerical method. The relation is given as

$$\mu = \frac{m_s \sqrt{\pi\nu}}{2} \frac{\Gamma\left(\frac{\nu}{2(\nu-1)}\right)}{\Gamma\left(\frac{1}{2(\nu-1)}\right)} q^{-\frac{\nu}{4(\nu-1)}} \times \frac{1}{1 - \sum_{n=1}^{\infty} \frac{\nu}{1+(2n+1)(\nu-1)} q^n b_n w_n}, \quad (\text{C5})$$

where the expansion is in terms of q ,

$$q = e^{-4(B+\Delta)\left(1-\frac{1}{\nu}\right)}; \quad (\text{C6})$$

$$\Delta = \frac{1}{2} \log(\nu-1) - \frac{\nu}{2(\nu-1)} \log \nu. \quad (\text{C7})$$

The coefficients b_n are given explicitly as

$$b_n = \frac{(-1)^n}{n!(n-1)!} \frac{\Gamma\left(\frac{n}{\nu}\right) \Gamma\left(\frac{3}{2} + \frac{n(\nu-1)}{\nu}\right)}{\Gamma\left(-\frac{n}{\nu}\right) \Gamma\left(\frac{3}{2} - \frac{n(\nu-1)}{\nu}\right)}, \quad (\text{C8})$$

and $w_n \equiv w_n(q)$ are provided implicitly through the linear system

$$w_n = \frac{1}{n} - \sum_{m=1}^{\infty} \frac{q^m}{m+n} b_m w_m. \quad (\text{C9})$$

Figure 9 shows how the above expansion, truncated at various orders of q , approaches (exponentially) to the TBA-computed values towards larger B , providing an important consistency check for the latter.

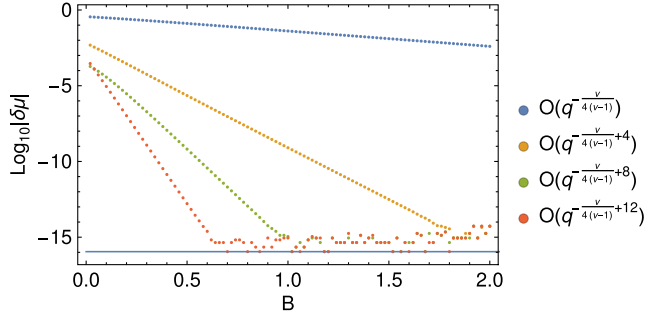


FIG. 9. Precision of various orders of the series expansion of Eq. (C5), as compared to TBA. The base-10 logarithm of MACHINEPRECISION is shown with a blue line.

APPENDIX D: DETAILS OF THE PERTURBATIVE CALCULATION

Using Eq. (60), normalizing the vertex operators in finite volume with the appropriate $(2\pi L^{-1})$ factors so that their normalization is consistent with Eq. (28),

$$\begin{aligned} \chi(q, i\omega)_1 = & \left(\frac{\tilde{m}}{4\pi}\right)^2 \frac{1}{N_c N_f \pi (4\pi)^2} \int_{-\infty}^{\infty} d\tau_1 \int_{-\infty}^{\infty} d\tau_2 \int_{-\infty}^{\infty} \int_{-\infty}^{\infty} dx_1 dx_2 \cdot \\ & \times \int_{-\infty}^{\infty} \int_{-\infty}^{\infty} dX dT e^{iqX + i\omega T} |z_1 - z_2|^{-2\alpha} \\ & \times \cos(2k_0(x_1 - x_2)) \cdot \\ & \times \left(\frac{1}{Z - z_1} - \frac{1}{Z - z_2} - \text{c.c.}\right) \left(\frac{1}{z_2} - \frac{1}{z_1} - \text{c.c.}\right), \end{aligned} \quad (\text{D1})$$

where $Z = T - iX$, $z_{1,2} = \tau_{1,2} - ix_{1,2}$ and α was defined in Eq. (61). We first perform the X and T integration of Eq. (D1). Using the residue theorem, we obtain

$$\begin{aligned} \chi(q, i\omega)_1 = & \left(\frac{\tilde{m}}{4\pi}\right)^2 \frac{1}{N_c N_f \pi (4\pi)^2} \beta^2 \\ & \times \int_{-\infty}^{\infty} d\tau_2 \int_{-\infty}^{\infty} d\tau_1 \int_{-\infty}^{\infty} \int_{-\infty}^{\infty} dx_1 dx_2 \\ & \times |z_1 - z_2|^{-2\alpha} \cos(2k_0(x_1 - x_2)) \left(\frac{1}{z_2} - \frac{1}{z_1} - \text{c.c.}\right) \\ & \times \frac{4\pi q}{q^2 + \omega^2} (e^{iqx_2 + i\omega\tau_2} - e^{iqx_1 + i\omega\tau_1}). \end{aligned} \quad (\text{D2})$$

We then change integration variables $x_1 \rightarrow x + x_2$, $\tau_1 \rightarrow \tau + \tau_2$ and integrate with respect to x_2 and τ_2 . This is again possible with the residue theorem. We arrive at

$$\begin{aligned} \chi(q, i\omega)_1 = & \left(\frac{\tilde{m}}{4\pi}\right)^2 \frac{1}{N_c N_f \pi (4\pi)^2} \frac{\beta^2}{q^2 + \omega^2} \frac{4\pi q}{q^2 + \omega^2} \frac{-16\pi q}{q^2 + \omega^2} \\ & \times \int_{-\infty}^{\infty} d\tau \int_{-\infty}^{\infty} dx \\ & \times (x^2 + \tau^2)^{-\alpha} \cos(2k_0 x) \sin^2\left(\frac{qx + \omega\tau}{2}\right). \end{aligned} \quad (\text{D3})$$

This integral can be evaluated analytically, and yields an explicit formula for general q , ω , leading to the result reported in Eq. (62).

-
- [1] J. Walecka, *Theoretical Nuclear and Subnuclear Physics* (Imperial College Press, London, 1995).
 - [2] G. A. Lalazissis, J. König, and P. Ring, *Phys. Rev. C* **55**, 540 (1997).
 - [3] B. D. Serot and J. D. Walecka, *Int. J. Mod. Phys. E* **06**, 515 (1997).
 - [4] A. Akmal, V. Pandharipande, and D. Ravenhall, *Phys. Rev. C* **58**, 1804 (1998).
 - [5] J. Carriere, C. J. Horowitz, and J. Piekarewicz, *Astrophys. J.* **593**, 463 (2003).
 - [6] P. Danielewicz, R. Lacey, and W. G. Lynch, *Science* **298**, 1592 (2002).
 - [7] E. Epelbaum, H.-W. Hammer, and U.-G. Meissner, *Rev. Mod. Phys.* **81**, 1773 (2009).
 - [8] R. Machleidt and D. Entem, *Phys. Rep.* **503**, 1 (2011).
 - [9] A. Kurkela, P. Romatschke, and A. Vuorinen, *Phys. Rev. D* **81**, 105021 (2010).
 - [10] A. Kurkela, E. S. Fraga, J. Schaffner-Bielich, and A. Vuorinen, *Astrophys. J.* **789**, 127 (2014).
 - [11] A. Kurkela and A. Vuorinen, *Phys. Rev. Lett.* **117**, 042501 (2016).
 - [12] I. Ghisoiu, T. Gorda, A. Kurkela, P. Romatschke, M. Säppi, and A. Vuorinen, *Nucl. Phys.* **B915**, 102 (2017).
 - [13] E. Annala, T. Gorda, A. Kurkela, and A. Vuorinen, *Phys. Rev. Lett.* **120**, 172703 (2018).
 - [14] T. Gorda, A. Kurkela, P. Romatschke, M. Säppi, and A. Vuorinen, *Phys. Rev. Lett.* **121**, 202701 (2018).
 - [15] E. Annala, T. Gorda, A. Kurkela, J. Nättilä, and A. Vuorinen, *Nat. Phys.* **16**, 907 (2020).
 - [16] T. Gorda, A. Kurkela, R. Paatelainen, S. Säppi, and A. Vuorinen, *Phys. Rev. Lett.* **127**, 162003 (2021).
 - [17] T. Gorda, A. Kurkela, R. Paatelainen, S. Säppi, and A. Vuorinen, *Phys. Rev. D* **104**, 074015 (2021).

- [18] L. McLerran and R. D. Pisarski, *Nucl. Phys.* **A796**, 83 (2007).
- [19] A. Andronic *et al.*, *Nucl. Phys.* **A837**, 65 (2010).
- [20] T. Kojo, Y. Hidaka, L. McLerran, and R. D. Pisarski, *Nucl. Phys.* **A843**, 37 (2010).
- [21] T. Kojo, R. D. Pisarski, and A. M. Tsvetlik, *Phys. Rev. D* **82**, 074015 (2010).
- [22] T. Kojo, Y. Hidaka, K. Fukushima, L. D. McLerran, and R. D. Pisarski, *Nucl. Phys.* **A875**, 94 (2012).
- [23] K. Fukushima and T. Kojo, *Astrophys. J.* **817**, 180 (2016).
- [24] L. McLerran and S. Reddy, *Phys. Rev. Lett.* **122**, 122701 (2019).
- [25] K. S. Jeong, L. McLerran, and S. Sen, *Phys. Rev. C* **101**, 035201 (2020).
- [26] D. C. Duarte, S. Hernandez-Ortiz, and K. S. Jeong, *Phys. Rev. C* **102**, 065202 (2020).
- [27] D. C. Duarte, S. Hernandez-Ortiz, and K. S. Jeong, *Phys. Rev. C* **102**, 025203 (2020).
- [28] S. Sen and N. C. Warrington, *Nucl. Phys.* **A1006**, 122059 (2021).
- [29] S. Sen and L. Sivertsen, *Astrophys. J.* **915**, 109 (2021).
- [30] T. Zhao and J. M. Lattimer, *Phys. Rev. D* **102**, 023021 (2020).
- [31] R. D. Pisarski, *Phys. Rev. D* **103**, L071504 (2021).
- [32] D. C. Duarte, S. Hernandez-Ortiz, K. S. Jeong, and L. D. McLerran, *Phys. Rev. D* **104**, L091901 (2021).
- [33] R. D. Pisarski, V. V. Skokov, and A. M. Tsvetlik, *Phys. Rev. D* **99**, 074025 (2019).
- [34] R. D. Pisarski, A. M. Tsvetlik, and S. Valgushev, *Phys. Rev. D* **102**, 016015 (2020).
- [35] R. D. Pisarski and F. Rennecke, *Phys. Rev. Lett.* **127**, 152302 (2021).
- [36] R. D. Pisarski and A. M. Tsvetlik, arXiv:2103.15835.
- [37] P. Azaria, R. Konik, P. Lecheminant, T. Palmi, G. Takacs, and A. Tsvetlik, *Phys. Rev. D* **94**, 045003 (2016).
- [38] V. Baluni, *Phys. Lett.* **90B**, 407 (1980).
- [39] P. J. Steinhardt, *Nucl. Phys.* **B176**, 100 (1980).
- [40] E. Cohen, Y. Frishman, and D. Gepner, *Phys. Lett.* **121B**, 180 (1983).
- [41] D. Gepner, *Nucl. Phys.* **B252**, 481 (1985).
- [42] Y. Frishman and J. Sonnenschein, *Phys. Rep.* **223**, 309 (1993).
- [43] A. Armoni, Y. Frishman, J. Sonnenschein, and U. Trittmann, *Nucl. Phys.* **B537**, 503 (1999).
- [44] R. Gopakumar, A. Hashimoto, I. R. Klebanov, S. Sachdev, and K. Schoutens, *Phys. Rev. D* **86**, 066003 (2012).
- [45] M. Isachenkov, I. Kirsch, and V. Schomerus, *Nucl. Phys.* **B885**, 679712 (2014).
- [46] D. Controzzi and A. M. Tsvetlik, *Phys. Rev. B* **72**, 035110 (2005).
- [47] A. J. A. James, R. M. Konik, P. Lecheminant, N. J. Robinson, and A. M. Tsvetlik, *Rep. Prog. Phys.* **81**, 046002 (2018).
- [48] A. B. Zamolodchikov and V. A. Fateev, *Yad. Fiz.* **43**, 1031 (1986) [*Sov. J. Nucl. Phys.* **43**, 657 (1986)], <https://inspirehep.net/literature/238357>.
- [49] G. I. Japaridze, A. A. Nersesian, and P. B. Wiegmann, *Nucl. Phys.* **B230**, 511 (1984).
- [50] A. B. Zamolodchikov, *Int. J. Mod. Phys. A* **10**, 1125 (1995).
- [51] A. G. Izergin, V. E. Korepin, and N. Y. Reshetikhin, *J. Phys. A* **22**, 2615 (1989).
- [52] E. Papa and A. M. Tsvetlik, *Phys. Rev. B* **63**, 085109 (2001).
- [53] R. M. Konik and P. Fendley, *Phys. Rev. B* **66**, 144416 (2002).
- [54] J. W. Holt, M. Rho, and W. Weise, *Phys. Rep.* **621**, 2 (2016).
- [55] K. Fukushima and C. Sasaki, *Prog. Part. Nucl. Phys.* **72**, 99 (2013).
- [56] W. E. Brown, J. T. Liu, and H.-c. Ren, *Phys. Rev. D* **62**, 054013 (2000).
- [57] D. Boyanovsky and H. J. de Vega, *Phys. Rev. D* **63**, 034016 (2001).
- [58] A. Ipp, A. Gerhold, and A. Rebhan, *Phys. Rev. D* **69**, 011901 (2004).
- [59] A. Gerhold, A. Ipp, and A. Rebhan, *Phys. Rev. D* **70**, 105015 (2004).
- [60] T. Schäfer and K. Schwenzer, *Phys. Rev. D* **70**, 054007 (2004).
- [61] M. Kitazawa, T. Kunihiro, and Y. Nemoto, *Phys. Lett. B* **631**, 157 (2005).
- [62] M. Kitazawa, T. Koide, T. Kunihiro, and Y. Nemoto, *Prog. Theor. Phys.* **114**, 117 (2005).
- [63] K. Pal and A. K. Dutt-Mazumder, *Phys. Rev. D* **84**, 034004 (2011).
- [64] S. P. Adhya, P. K. Roy, and A. K. Dutt-Mazumder, *Phys. Rev. D* **86**, 034012 (2012).
- [65] A. D. Linde, *Phys. Lett.* **96B**, 289 (1980).
- [66] D. J. Gross, R. D. Pisarski, and L. G. Yaffe, *Rev. Mod. Phys.* **53**, 43 (1981).
- [67] T. Appelquist and R. D. Pisarski, *Phys. Rev. D* **23**, 2305 (1981).
- [68] R. Jackiw and S. Templeton, *Phys. Rev. D* **23**, 2291 (1981).
- [69] K. Kajantie, M. Laine, K. Rummukainen, and M. E. Shaposhnikov, *Nucl. Phys.* **B503**, 357 (1997).
- [70] K. Kajantie, M. Laine, K. Rummukainen, and Y. Schroder, *Phys. Rev. Lett.* **86**, 10 (2001).
- [71] K. Kajantie, M. Laine, K. Rummukainen, and Y. Schroder, *Phys. Rev. D* **67**, 105008 (2003).
- [72] A. Hietanen, K. Kajantie, M. Laine, K. Rummukainen, and Y. Schroder, *Phys. Rev. D* **79**, 045018 (2009).
- [73] J. B. Kogut, D. K. Sinclair, S. J. Hands, and S. E. Morrison, *Phys. Rev. D* **64**, 094505 (2001).
- [74] C. R. Allton, S. Ejiri, S. J. Hands, O. Kaczmarek, F. Karsch, E. Laermann, and C. Schmidt, *Phys. Rev. D* **68**, 014507 (2003).
- [75] C. R. Allton, M. Doring, S. Ejiri, S. J. Hands, O. Kaczmarek, F. Karsch, E. Laermann, and K. Redlich, *Phys. Rev. D* **71**, 054508 (2005).
- [76] S. Hands, S. Kim, and J.-I. Skullerud, *Eur. Phys. J. C* **48**, 193 (2006).
- [77] S. Hands, S. Kim, and J.-I. Skullerud, *Phys. Rev. D* **81**, 091502 (2010).
- [78] S. Hands, P. Kenny, S. Kim, and J.-I. Skullerud, *Eur. Phys. J. A* **47**, 60 (2011).
- [79] S. Hands and P. Kenny, *Phys. Lett. B* **701**, 373 (2011).
- [80] S. Cotter, P. Giudice, S. Hands, and J.-I. Skullerud, *Phys. Rev. D* **87**, 034507 (2013).

- [81] S. Hands, S. Kim, and J.-I. Skullerud, *Phys. Lett. B* **711**, 199 (2012).
- [82] A. Amato, P. Giudice, and S. Hands, *Eur. Phys. J. A* **51**, 39 (2015).
- [83] V. G. Bornyakov, V. V. Braguta, E. M. Ilgenfritz, A. Y. Kotov, A. V. Molochkov, and A. A. Nikolaev, *J. High Energy Phys.* 03 (2018) 161.
- [84] N. Y. Astrakhantsev, V. G. Bornyakov, V. V. Braguta, E. M. Ilgenfritz, A. Y. Kotov, A. A. Nikolaev, and A. Rothkopf, *J. High Energy Phys.* 05 (2019) 171.
- [85] T. Boz, P. Giudice, S. Hands, and J.-I. Skullerud, *Phys. Rev. D* **101**, 074506 (2020).
- [86] V. V. Braguta, A. Y. Kotov, and A. A. Nikolaev, *JETP Lett.* **110**, 1 (2019).
- [87] K. Iida, E. Itou, and T.-G. Lee, *J. High Energy Phys.* 01 (2020) 181.
- [88] J. Wilhelm, L. Holicki, D. Smith, B. Wellegehausen, and L. von Smekal, *Phys. Rev. D* **100**, 114507 (2019).
- [89] V. G. Bornyakov, V. V. Braguta, A. A. Nikolaev, and R. N. Rogalyov, *Phys. Rev. D* **102**, 114511 (2020).
- [90] T. Furusawa, Y. Tanizaki, and E. Itou, *Phys. Rev. Research* **2**, 033253 (2020).
- [91] K. Iida, E. Itou, and T.-G. Lee, *Prog. Theor. Exp. Phys.* **2021**, 013B05 (2021).
- [92] A. Begun, V. G. Bornyakov, N. V. Gerasimeniuk, V. A. Goy, A. Nakamura, R. N. Rogalyov, and V. Vovchenko, [arXiv:2103.07442](https://arxiv.org/abs/2103.07442).
- [93] V. G. Bornyakov and R. N. Rogalyov, *Int. J. Mod. Phys. A* **36**, 2044032 (2021).
- [94] V. G. Bornyakov, A. A. Nikolaev, R. N. Rogalyov, and A. S. Terentev, *Eur. Phys. J. C* **81**, 747 (2021).
- [95] K. Ishiguro, K. Iida, and E. Itou, [arXiv:2111.13067](https://arxiv.org/abs/2111.13067).
- [96] D. V. Deryagin, D. Yu. Grigoriev, and V. A. Rubakov, *Int. J. Mod. Phys. A* **07**, 659 (1992).
- [97] K. Fukushima, J. M. Pawłowski, and N. Strodthoff, [arXiv:2103.01129](https://arxiv.org/abs/2103.01129).
- [98] V. Braguta, E. M. Ilgenfritz, A. Y. Kotov, A. Molochkov, and A. Nikolaev, *Phys. Rev. D* **94**, 114510 (2016).
- [99] R. D. Pisarski, F. Rennecke, A. Tsvetik, and S. Valgushev, *Nucl. Phys. A* **1005**, 121910 (2021).
- [100] A. Bzdak, S. Esumi, V. Koch, J. Liao, M. Stephanov, and N. Xu, *Phys. Rep.* **853**, 1 (2020).
- [101] B. Lucini and M. Panero, *Phys. Rep.* **526**, 93 (2013).
- [102] B. Lucini and M. Panero, *Prog. Part. Nucl. Phys.* **75**, 1 (2014).
- [103] A. W. Overhauser, *Phys. Rev. Lett.* **4**, 415 (1960).
- [104] A. B. Migdal, *Rev. Mod. Phys.* **50**, 107 (1978).
- [105] D. B. Kaplan and A. E. Nelson, *Phys. Lett. B* **175**, 57 (1986).
- [106] G. E. Brown and M. Rho, *Nucl. Phys. A* **596**, 503 (1996).
- [107] J. B. Kogut, M. A. Stephanov, and D. Toublan, *Phys. Lett. B* **464**, 183 (1999).
- [108] J. B. Kogut, M. A. Stephanov, D. Toublan, J. J. M. Verbaarschot, and A. Zhitnitsky, *Nucl. Phys. B* **582**, 477 (2000).
- [109] D. Son and M. A. Stephanov, *Phys. At. Nucl.* **64**, 834 (2001).
- [110] N. Astrakhantsev, V. Braguta, E.-M. Ilgenfritz, A. Kotov, and A. Nikolaev, *Phys. Rev. D* **102**, 074507 (2020).
- [111] R. D. Pisarski and F. Rennecke, *Phys. Rev. D* **101**, 114019 (2020).
- [112] D. G. Yakovlev, A. D. Kaminker, O. Y. Gnedin, and P. Haensel, *Phys. Rep.* **354**, 1 (2001).
- [113] D. G. Yakovlev and C. J. Pethick, *Annu. Rev. Astron. Astrophys.* **42**, 169 (2004).
- [114] D. Page, J. M. Lattimer, M. Prakash, and A. W. Steiner, *Astrophys. J. Suppl. Ser.* **155**, 623 (2004).
- [115] D. Page, M. Prakash, J. M. Lattimer, and A. W. Steiner, *Phys. Rev. Lett.* **106**, 081101 (2011).
- [116] P. S. Shternin, D. G. Yakovlev, C. O. Heinke, W. C. G. Ho, and D. J. Patnaude, *Mon. Not. R. Astron. Soc.* **412**, L108 (2011).
- [117] A. Y. Potekhin, J. A. Pons, and D. Page, *Space Sci. Rev.* **191**, 239 (2015).
- [118] A. Schmitt and P. Shternin, *Astrophysics and Space Science Library* **457**, 455 (2018).
- [119] N. Iwamoto, *Ann. Phys. (N.Y.)* **141**, 1 (1982).
- [120] J. B. Zuber and C. Itzykson, *Phys. Rev. D* **15**, 2875 (1977).
- [121] M. C. Abbott, Z. Bajnok, J. Balog, A. Hegedús, and S. Sadeghian, *J. High Energy Phys.* 05 (2021) 253.
- [122] W. H. Press, S. A. Teukolsky, W. T. Vetterling, and B. P. Flannery, *Numerical Recipes 3rd Edition: The Art of Scientific Computing*, 3rd ed. (Cambridge University Press, USA, 2007).